Doctoral Dissertation
博士論文

Elucidation of cell types of maternal microchimeric cell population in mice fetus

（胎児に移入する母由来細胞の細胞種の解明）

A Dissertation Submitted for the Degree of Doctor of Philosophy
December 2021
令和 3 年 12 月 博士（理学）申請

Department of Biological Sciences, Graduate School of Science,
The University of Tokyo
東京大学大学院理学系研究科
生物科学専攻

Kana Fujimoto
藤本　香菜

Table of Contents

Abstract **4**

Chapter 1 General Introduction **7**

1.1 MATERNAL MICROCHIMERIC (MMC) CELLS. 8

1.2 POSSIBLE RELATIONSHIPS BETWEEN MMC CELLS AND VARIOUS PHENOMENA 9

1.3 TECHNICAL LIMITATIONS IN ANALYZING MMC CELLS. 11

1.4 BIOLOGICAL ROLES OF MMC CELL. 12

Chapter 2 Development of MMc cell isolation system **14**

2.1 INTRODUCTION 15

2.2 MATERIAL AND METHODS 16

2.2.1 MMc cell isolation method *16*

2.2.2 Whole embryo transparent by CUBIC *18*

2.3 RESULTS 24

2.3.1 Development of whole embryonic MMc cell detection protocol *24*

2.3.2 An attempt to reveal the distribution of MMc cells in the whole embryo *25*

2.4 DISCUSSION 28

2.4.1 Successful development of MMc cell isolation method *28*

2.4.2 Small difference in the amino acid sequences of GFP interfered with successful immunostaining of GFP. *28*

2.5 FIGURES AND TABLES 30

Chapter 3 Isolation of MMc cells from whole-embryonic mice samples and comparison of its numbers **49**

3.1 Introduction 50

3.2 Material and Methods 51

3.3 Results 53

3.4 Discussion 55

3.5 Figures and Tables 58

Chapter 4 MMc cell type estimation by utilizing single cell RNA-seq 64

4.1 Introduction 65

4.2 Material and Methods 66

4.3 Results 73

4.4 Discussion 78

4.5 Figures and Tables 81

Chapter 5 General Discussion 96

5.1 Number of MMc cells in a whole embryo 97

5.2 Variety of MMc cell types in a whole embryo 98

5.3 Relationships between MMc cells and various phenomena 100

Acknowledgements 102

References 104

Abstract

During pregnancy in placental mammals, small numbers of maternal cells (maternal microchimeric cells, or MMc cells) migrate into the fetus and persist decades, or perhaps for the rest of their lives. Given this inheritance, microchimerism can also be regarded as cell-level epigenetics. While migration of MMc cells into fetus is considered to occur in all pregnant cases, higher frequencies of MMc cells are reported in variety of phenomena, such as immune tolerance, tissue repair, and autoimmune diseases. However, it is not known what makes MMc cells involved in such a variety of phenomena. One possibility would be that number of MMc cells may differ among different individual embryos, however, no study so far has verified this possibility. Alternatively, it is also possible that repertoire of cell types and distribution of MMc cells differ in each individual embryo, contributing to the variety of phenomena.

Here, for the first time, I developed a whole embryonic detection method for MMc cells using transgenic mice and counted live MMc cells in each individual embryo. Using this technique, I found that the number of MMc cells was comparable in most of the analyzed embryos; however, around 500 times higher number of MMc cells was detected in one embryo at the latest developmental stage. This result suggests that the number of MMc cells could largely differ in rare cases with unknown mechanisms. In addition, I also revealed repertoire of MMc cell types in whole embryos of early phase of MMc cell migration, namely E14.5 in mice, and estimated the cell types using single cell RNA-seq, gene expression profiling technique. In addition to the immune cell types which were often reported in previous studies, I found that there are other cell types such as cells that are considered to be terminally differentiated, and under proliferation. These imply that embryos receive variety of non-inherited maternal

antigens (NIMAs) through MMc cells, and could be contributing to immunological tolerance against maternal antigens. In addition, terminally differentiated maternal cell reported in some case of patients could directly be contributed by these differentiated cells, rather than differentiation from undifferentiated stem MMc cells. Furthermore, I found that all the isolated MMc cells commonly expressed genes of two transmembrane proteins that are known to be involved in cell migrations. This provides possible basis for understanding how MMc cells migrate from maternal side to fetal side.

These data provide a hint toward understanding the biological roles of MMc cells and mechanisms underlying the variety of apparently inconsistent MMc-related phenomena.

Chapter 1　General Introduction

1.1 Maternal microchimeric (MMc) cells.

Generally, animal body consists of its own cells that divide from a single fertilized egg (except for symbiotic microorganisms in the body). However, this does not apply to placental mammals, including humans and mice, as small numbers (around 1 in 100,000 cells in humans) of maternal cells obtained during pregnancy exist in our body (1). This phenomenon is called maternal microchimerism (MMc), which signifies a chimera of our own cells and small numbers of genetically and immunologically non-self, maternal cells (2)(3)(4). These maternal microchimeric cells (MMc cells) migrate into the body via the placenta (and through milk after birth) (5) and are retained for decades after birth(1)(6)(7). Although there are other cases of "non-self cell contamination" in human, such as organ transplant and blood transfusion, I focused only on MMc cells.

Placenta is generally thought to be a selective physical barrier between mother and fetus. While exchanging gases, supplies nutrients and antibodies from the mother to the fetus, it prevents blood and tissue exchange to each other. However, cell migration between mother and fetus during pregnancy has been observed in various species of placental mammals, such as mice, primates, dogs, cows and so on (8). Since cells of maternal origin were also identified in the blood contained in the umbilical cord, maternal cell migration were predicted to occur through the placenta and umbilical cord (9)(10). However, the exact mechanism of maternal cell migration through the placenta still remains to be clarified. In human, fetal cell migration between mother and fetus has been suggested to start from 7-16 weeks, the time when placentation begins in humans (11). In the meanwhile, it starts even

before the time of placentation in mice (12), and MMc cells can be detected as early as E12.5–E13.5 in mice (13)(14), which is period of active morphogenesis. In addition, breast milk has also been verified to be an alternative route for MMc cells to migrate into fetus (5)(15)(16).

MMc cells have been identified in various organs before and after birth, and identified cell types include cardiac myocytes, keratinocytes, bile duct epithelial cells, insulin secreting cells and so on (13)(17). Since MMc cells exist in many organs and tissues for a long period of time, it is considered that MMc cells contain cells of stem cell lineage and acquire stem-cell niches after migration. Consistent with this, hematopoietic stem cells of MMc cells have been found in the bone marrow of offspring (18). In the meanwhile, there are many remaining questions, such as whether tissue-specific cell types other than stem cells migrate, how non-self-derived cells acquire a stem-cell niche, and whether differentiated cells that are not of stem cell lineage can acquire the niche after their migration. Although these questions are not all answered in this study, they are very important to be answered to understand the kinetics and biological roles of MMc cells.

1.2 Possible relationships between MMc cells and various phenomena.

Previous studies have suggested possible roles of both beneficial and harmful aspects of MMc cells, based on the findings that MMc cells were enriched in various phenomena. Beneficial aspects include establishment of immune tolerance against noninherited maternal antigens in offspring (19)(20)(21)(22) and potential contribution to tissue repair

(6)(7)(23)(24). In the meanwhile, possible harmful effects include contributions to the pathogenesis or deterioration of some inflammatory diseases and congenital malformations (25)(26)(27)(28)(29). These studies imply that MMc cells could be involved in opposing phenomena with unknown mechanisms. Meanwhile, it could merely a result of *post hoc* expansion of MMc cells which took place after the onset of the disease or tissue repair. I thus hypothesized and decided to test if the number of MMc cells migrated in fetus differ among individuals from the early phase of MMc cell migration. Consistent with this idea, the frequency of MMc cells seems to differ not only among different cases but also among patients with the same disease or even among control groups (6)(26). Some patients with type I diabetes, for example, had approximately 500 MMc cells per 100,000 host cells (estimated using the amount of DNA equivalents), whereas others had undetectable levels of MMc cells. Similarly, a very high frequency of MMc cells was also found in an unaffected sibling, showing 153 MMc cells per 100,000 host cells, whereas most of the unaffected siblings showed 3.5 cells per 100,000 cells (6). In this study, I therefore decided to test if there are differences in the number of MMc cells among embryos of normal pregnancies.

In addition to the MMc cell number, it is also possible that repertoires of MMc cell types differ among embryos, and this contributes to variety of phenomena. In type 1 diabetes, MMc cells were identified as β cell at pancreas with insulin signal positive. From this result, it was suggested that MMc cells can help the child, at least partially, to regenerate their damaged β cells. On the other hand, at inflammatory portion of liver in the patient with biliary atresia, enriched numbers of maternal cytotoxic T cells are found. Considering that this cell type is known to have a function to attack the immunologically non-self antigens,

and frequency of MMc cells tends to be higher in biliary atresia patients when compared with other diseased control patients, it is possible that MMc cells could have contributed or deteriorated the inflammatory aspect of this disease. However, these studies have been shown in human cases, and there is no direct evidence showing MMc cells can cause these symptoms. With this perspective, animal experiment systems that can clearly test these hypotheses were awaited. Moreover, no study so far has analyzed the overall composition of MMc cell population.

Together, I hypothesized and tested if there are differences in the number and cell-type repertoire of MMc cells among individual embryos, which could lead to seemingly inconsistent phenomena (immunological tolerance, tissue repair, and inflammatory disease).

1.3 Technical limitations in analyzing MMc cells.

To test if the number of MMc cells differ among embryos, I have developed an animal experimental system to overcome the major limitations in previous approaches.

First, previous studies focused only on MMc cells of a limited number of tissues and organs, and the number in whole embryo was unclear. This imply that different numbers of MMc cells reported in previous studies could merely represent a local accumulation of MMc cells in the tissue of focus, while the overall number of MMc cells in the fetus do not differ among the different individuals. In addition, many studies used qPCR technique to count MMc cells by detecting maternal specific gene, such as MHC type or sex chromosomes. Although this qPCR-based approach is useful for detecting MMc cells which are often low in frequency, the drawback is that it also detects cell free-DNA of maternal origin, being unable

to accurately count the MMc cells. Secondly, no study has ever identified whole picture of MMc cell types migrated into the embryo, as previous studies used limited numbers of cell type specific markers. While accumulating numbers of studies were done in this way, there could be missing type of cells that were not targeted, and what is more, these do not tell us the cell type balance or repertoire of MMc cell types migrated into the fetus. Thirdly, as I discussed above, most of previous studies focused only on MMc cells from a limited number of tissues and organs, so it is unclear whether the distribution of MMc cells differs between individual embryos or not.

By overcoming these technical difficulties and clarifying both MMc cell number and cell type repertoire from whole embryo, I aim to obtain a hint toward the relationship between MMc cells and seemingly inconsistent, various phenomena.

1.4 Biological roles of MMc cell.

Some pioneering studies showed biological significance of MMc cells, especially their contribution to immunological tolerance between mother and fetus. Kinder *et al.* (19) showed that maternal cells (especially maternal regulatory T cells) contribute to establishment of tolerance for non-inherited maternal antigen (NIMA), and this further helps her daughter to establish a successful pregnancy when the daughter become pregnancy with a fetus having an antigen similar to the non-inherited maternal antigen. In addition, Bracamonte-Baran *et al.* (30) showed that maternal MHC-antigen complex can be transported into the child's dendritic cells by the dendritic cells of maternal origin and this can suppress the child's T cell activity. Thirdly, by establishing tolerance for maternal

antigens, even if the child don't have the non-inherited maternal antigens in their genomes, organ transplant success rates increase (31). Based on these facts, it can be said that maternal cells, especially immune system-related maternal cells, should be considered as an important regulator of fetal immune system. However, considering the possible involvement to inflammatory disease as described in the introductory section, the role as the immune system regulator requires further investigation.

In addition to immune system-related cell types, but also other cell types, such as stem cells could influence the children's health even long after birth. For example, existence of maternal hematopoietic stem cells in bone marrow (18) and mesenchymal stem cells of maternal origin (22) are known. This implies the potential medication for the children's health could be developed by controlling the number and cell types during pregnancy or breast-feeding. Revealing the cell type repertoire and migrated cell number are also important with this regard.

Chapter 2　Development of MMc cell isolation system

2.1 Introduction

As discussed in Chapter 1, low frequency of MMc cells is the main barrier for detecting maternal cells, and this hindered scientists from clarifying the number and distribution of MMc cells in whole embryo. In addition, there has been no research which revealed overall repertoire of MMc cell types, but only focused on specific cell types. Therefore, we still do not know whether MMc cell population (cell number, cell type and cell distribution) differ between individuals or not. To answer this question, I decided to develop efficient isolation technique from whole mouse embryo, and count MMc cells. In addition, I further tried to analyze MMc cell distributions in an embryo. For this, I tried making the whole embryo transparent by CUBIC reagent. In this chapter, I will discuss the development and efficiency of MMc isolation technique from the mouse whole embryo, and further the trial experiments of revealing MMc cell distribution in mouse embryo which were made into transparent using CUBIC reagent.

2.2 Material and Methods

2.2.1 MMc cell isolation method

Mouse strains

The inbred strains, BALB/cByJJcl and C57BL/6JJcl were obtained from Clea Japan. Green fluorescent protein (GFP) expressing mice, C57BL/6-Tg(CAG-EGFP)C14-Y01-FM131Osb was obtained from RIKEN BioResource Research Center (RBRC), which was developed by Okabe M. *et al.* (32) and genotyping was performed according to the instructions provided by RBRC using polymerase chain reaction (PCR). To obtain GFP heterozygous female mice, BALB/c female mice were mated with GFP homozygous male mice. To obtain wild type fetus with GFP positive MMc cells, GFP heterozygous female mice were mated with BALB/c male mice and only fetuses without GFP genes were used for experiments (Fig 1, 2).

Preparation of cell suspensions from whole embryo

To obtain suspensions of dissociated cells from the whole embryo, GFP^- embryos (identified by the absence of fluorescence using GFP excitation flashlight while embryos are in amnion) were dissected. In brief, pregnant females were first sacrificed and uteruses were cut out to obtain embryos with amnion, and placed in cold phosphate-buffered saline. After transferring the embryo to a new cold phosphate-buffered saline, amnions were removed from embryos, followed by a cut of the umbilical cord. Embryos were then washed with cold phosphate-buffered saline 3 times by picking the fetal side of remaining umbilical cord (to avoid possible contamination of maternal cells during

this process). To obtain dissociated cells, each embryo was first minced using a scissors and further dissociated by incubating in solution with 1 mg/ml collagenase D (Roche), 2.4 mg/ml Dispase (gibco), 100 U/ml DNase I (Roche) in Hanks' balanced salt solution (HBSS) (+)+3% Fetal bovine serum (FBS) for 20 min at 37 ℃. This enzyme cocktail was made by referring to Mass E *et al.* (33). The minced tissues were then filtered by squeezing into 100-μm cell strainers using the rubber part of the syringe (Rough Filtration). The filtered samples were centrifuged at 1,300 r.p.m. for 7 min at 4℃ followed by Ammonium-Chloride-Potassium (ACK) lysis buffer treatment for 6 min at r.t.. After removing erythrocytes, cold (on-ice) Fluorescence-activated cell sorting (FACS) buffer (HBSS(-), 0.5% Bovine serum albumin (BSA), 2mM Ethylene diamine tetra-acetic acid (EDTA)) was added to the cell suspension and centrifuged again with the same condition (1,300 r.p.m. for 7 min at 4 ℃). To generate single-celled suspension, the cell suspension was filtered again with 70-μm cell strainers (Finer Filtration). The number of cells in the cell suspension was counted and adjusted to 1.0×10^7 cells/ml concentration for the sorting process. For the control data for validating cell survival rate, cell suspension obtained from adult spleen was generated.

Evaluation of MMc isolation method by rough/finer filtrations and live cell ratio

Cell strainers (100-μm and 70-μm, Falcon) were used for both of the rough and finer filtrations. Whether or not the aggregation after the filtration mainly consists of dead cells were evaluated by trypan blue staining (100 μl trypan blue to the 5 ml cell suspension). Ratio of live cells were further analyzed with FACS (BD AriaIIIu) with Propidium iodide (PI) (Dojindo) staining.

2.2.2 Whole embryo transparent by CUBIC

Mouse strains

The same GFP$^+$ transgenic line to observe MMc cells in a whole embryo was used for this experiment. The inbred strains, BALB/cByJJcl and C57BL/6JJcl were obtained from Clea Japan. GFP expressing mice, C57BL/6-Tg(CAG-EGFP)C14-Y01-FM131Osb was obtained from RIKEN BioResource Research Center (RBRC), which was developed by Okabe M. *et al.* (32) and genotyping was performed according to the instructions provided by RBRC using PCR. To obtain GFP heterozygous female mice, BALB/c female mice were mated with GFP homozygous male mice. To obtain wild type fetus with GFP positive MMc cells, GFP heterozygous female mice were mated with BALB/c male mice and only fetuses without GFP genes were used for experiments. Fetuses in the pregnant C57BL/6JJcl female mice were used as negative controls for the MMc cell distribution experiment.

As a technical positive control for staining system, I used an adult (4-month-old) BALB/cByJJcl mouse's brain and GFP heterozygous female mouse's brain. This GFP heterozygous female mouse was obtained by mating C57BL/6-Tg(CAG-EGFP)C14-Y01-FM131Osb male mouse with BALB/cByJJcl female mouse.

Creation of transparent whole mice embryo sample

I followed the protocol of Clear, Unobstructed Brain/Body Imaging Cocktails and Computational analysis (CUBIC) (34)(35). Briefly, pregnant GFP heterozygous females were first sacrificed and uteruses were cut out to obtain embryos with amnion, and placed

in cold phosphate-buffered saline (PBS). After transferring the embryo to a new cold phosphate-buffered saline (PBS), the absence of fluorescence of the embryos were confirmed by using GFP excitation flashlight while embryos are in amnion. Then, amnions were removed from embryos, while the umbilical cords were un-touched, still connected to the fetus to avoid bleeding from embryos because it is considered that fetal blood is one of the most MMc cell containing organs. GFP negative embryos were fixed by 4% Paraformaldehyde (PFA) in PBS twenty four hours at 4℃. After fixation, 3 times PBS washes were conducted for 2 hours each. Washed embryos were transferred into 50% of CUBIC-L liquid (Tissue-Clearing Reagent CUBIC-L, TCI, T3740, was diluted with purified water into 50%) and incubated overnight at 37℃ by rotating, and then transferred again into 100% CUBIC-L liquid and incubated for 2~3 days at 37℃ by rotating and changing the liquid to fresh one every day as the lipid removal treatment. After de-lipidation, the embryos were washed in PBS 3 times 2 hours each. As the staining process, RedDot2, a cell membrane-impermeable dye and near-infrared fluorescent nuclear staining reagent, was used for nuclear staining to identify the cell position in the whole embryos. RedDot2 is known to be suitable for nuclear staining of dead cells. (I did not use PI for nuclei staining because PI absorbs green wavelength and it is not suitable combination with GFP. I also did not use DAPI [4',6-diamidino-2-phenylindole], which is commonly used blue fluorescent dye for nuclear staining of tissue immunostaining. The reasons are that because of the PFA fixation, the embryo sample turns yellowish and yellow absorb blue wavelength, and RedDot2 has superior thermal and photostability properties compared to DAPI.) RedDot2 was diluted in 1:100 in 4 ml

PBS, and embryos were incubated in this staining liquid for 3~4 days at 37°C by rotating with darken situation. After staining, the embryos were washed in PBS 3 times 2 hours each at room temperature by rotating with darken situation. After washing, as refractive index (RI) matching process, the embryos were transferred into 50% of CUBIC-R+ liquid (Tissue-Clearing Reagent CUBIC-R+(M), TCI, T3741, was diluted with purified water into 50%) and incubated overnight at room temperature by rotating under dark condition. Samples were then transferred again into 100% CUBIC-R+ liquid and incubated for 2~3 days at room temperature by rotating under dark condition, changing the liquid to fresh one every day during the lipid removal treatment.

After RI matching process, placenta was cut off and samples were transferred into enough amount of oil (which was evacuated for 5 minutes and its RI = 1.51), and I conducted the 3D observation with light sheet microscope (Olympus, Laser = 488 nm and 639 nm). Observation software was Macro 3D Imaging System (Exposure time (ms): 500 for 488 nm, 300 for 639 nm. Binning: 1x1. Gain: 16-bit (low noise & high well capacity). Zoom: 1.6x to 2.0x. Sequence: Merge ON/OFF: By Max Intensity. Incretment (μm): 10. Z-Scan Stepsize (μm): 10.) After taking pictures by light sheet microscope, I tried to identified MMc cells in the whole body of a fetus by overlapping the GFP signals and Red signals from nuclei with the analyzing software Imaris and ImageJ(1.52K Java 1.8.0_172).

Protocol for technical test of immunostaining

Before detecting the GFP positive cells by light sheet microscope observation, I constructed the experiments to enhance the GFP signals by immunostaining using anti-

GFP antibodies. To find the most suitable anti-GFP antibodies, I chose several monoclonal anti-GFP antibodies (Table 1). Since the gradient of the antibody concentration is important for penetration into three-dimensional tissues, monoclonal antibodies are suitable, rather than polyclonal antibodies. As the technical positive control for staining, I used anti-NeuN antibody (Table 1), which specifically recognizes the DNA-binding neuron-specific protein NeuN which exists in most central nerve system and peripheral nerve system, because this experiment referred (35). Therefore, for staining test, I used 2-dimensional tissue slices produced as frozen section by slicing the dilapidated adult mouse cerebellum in a sagittal way.

Frozen sections of an adult mouse cerebellum

To test if GFP can be detected through anti-GFP antibodies, I compared the staining levels between the brain tissues with and without GFP expression. Frozen sections of adult mouse cerebellum were prepared as bellow, and this protocol also referred (35). GFP heterozygous (expressing GFP in the whole body) female mouse and wild type (the inbred strains, BALB/cByJJcl) female mouse were first anesthetized by exposure to isoflurane and then transcardially perfused with 10 ml of cold PBS followed by 20 ml of 4% PFA in PBS. After cutting the head and removing the remain blood from the head, the cutting side of the head was immersed by 4% PFA in PBS for 30-60 min. Then, after confirming that the blood vessels were not observed through the skull, the brain was excised from the skull and only the cerebellum was transferred into the fresh 4% PFA in PBS as postfixation for 16 hours at 4℃ under shaking condition. After fixation, sample cerebellums were washed in PBS 3 times for 2 hours each. For de-

lipidation, washed cerebellums were transferred into 50% of CUBIC-L liquid (Tissue-Clearing Reagent CUBIC-L, TCI, T3740, was diluted with purified water into 50%) and incubated overnight at 37°C by rotating, and then transferred into 100% CUBIC-L liquid and incubated 2 days at 37°C by rotating. After de-lipidation, the embryos were washed in PBS 3 times 2 hours each. Washed cerebellums were transferred into 40% sucrose in PBS and immersed overnight at 4°C under shaking condition. After confirming the tissue was immersed, the tissue was embedded into O.C.T. compound (SAKURA) and sliced by cryostat (CM3050S, Leica) for 50 μm at -20°C both for OT and CT. Sliced sections were floated into PBS for removing O.C.T. compound and kept at 4°C until used for staining experiments.

Immunostaining experiment

Firstly, as the primary antibodies, anti-GFP antibodies and mouse monoclonal anti-NeuN antibody (MAB377) IgG1 were diluted by PBST [PBS 0.1% (v/v) Triton X-100]. Then, de-lipidated and sliced cerebellum sections were stained for primary antibodies overnight at 32°C under dark and shaking condition, followed by 2 times PBS wash for 10 min at room temperature under dark and shaking condition. Washed sections were stained by secondary antibody (Goat anti-mouse IgG (H+L) Highly Cross-Absorbed Secondary Antibody, Alexa Fluor 568) and DAPI for nuclei staining. The secondary antibody (Table 2) was diluted with PBST at 1:1000 [PBS 0.1% (v/v) Triton X-100], and DAPI was diluted with PBST at 1:500. Sections were incubated in the secondary antibody liquid for 2 hours at 32°C under dark and shaking condition, followed by 3 times PBS wash for 10 min at room temperature under dark and shaking

condition. The stained sections were mounted on slide grasses and observed by fluorescence confocal microscopy (Zeiss LSM710, 488 laser for tissue GFP observation, 561 laser for stained signal observation, and 405 laser for DAPI observation) to check the intense of GFP signal.

ImageJ (ImageJ 1.53a) was used to compare the signal intensities of sections. Maximum displayed value of Brightness/Contrast was adjusted as 100 for NeuN stained sections, 152 for each anti-GFP antibody stained sections, and 255 for GFP expressed by the tissue itself. To confirm the enhancement by staining, I compared GFP signals from tissue itself and stained signals by setting Laser power as 10.0 and Gain as 780 in fluorescence confocal microscopy (Zeiss LSM710) and didn't change the Brightness/Contrast conditions.

Comparison of amino acid sequences of GFP

All GFP nucleotide sequences (Table 3) were translated into amino acid sequences by Expasy. Then, the 5'3' Frame 1 sequences of each GFP were compared in their similarity by Needle (version 6.6.0, EMBOSS).

2.3 Results

2.3.1 Development of whole embryonic MMc cell detection protocol

Development of cell dissociation method

To identify maternal cells from the whole embryo, we took advantage of the green fluorescent protein (GFP) mouse strain. In brief, by crossing female mice heterozygous for the GFP locus ($GFP^{+/-}$) with wild-type male mice, I obtained wild-type fetuses ($GFP^{-/-}$) with GFP-carrying MMc cells (Fig 1, 2). Wild-type ($GFP^{-/-}$) embryos harboring $GFP^{+/-}$ MMc cells were then carefully dissected from their mother by repeated wash processes (three times with phosphate-buffered saline) and subjected to protease (trypsin) digestion, followed by two rounds (rough and fine) of physical filtration using cell strainers to dissociate cells.

The method performs well for developmental stages E12.5 to E15.5

I then analyzed which developmental stage of the mouse would be best suited for efficient isolation of MMc cells. Previous studies demonstrated that MMc cells can be detected as early as E12.5–E13.5 in mice (13)(14), and bi-directional trafficking of MMc cells is often considered to increase throughout gestation, peaking at parturition (36). Thus, I decided to target the developmental stages from E12.5 to E18.5. While later developmental stages are expected to have more MMc cells (36), dissociating cells would be more difficult because of the solid tissues enriched with extracellular matrices. As expected of the rough filtration process, minced samples from later developmental stages (E16.5 and E18.5) tended to retain more debris (presumably bones and tendons) after the filtration process

compared with earlier stages (Fig 3, 4). In contrast, the samples from earlier stages (E12.5–E15.5) were digested relatively easily by the filtering process. For the finer filtration process, although samples from all stages retained some aggregates, a relatively larger amount remained in E16.5 and E18.5 samples. After staining the pre-filtered sample with trypan blue, the filtered cells were unstained, while aggregates were stained blue (Fig 5), suggesting that they mainly consisted of dead cells or dead cells with extracellular matrices. The filtered cells were then analyzed for the ratio of live cells using PI markers and FACS (Fig 6). These results indicated that the ratio of live cells was comparable with that in control samples from the spleen, suggesting that a fair number of live cells can be obtained following my dissociation protocol. Considering that the aggregates remained after the two filtering processes for the late-stage samples (E16.5 and E18.5), it would be reasonable to conclude that this method is best suited for stages E12.5–E15.5, obtaining the maximum number of live cells.

2.3.2 An attempt to reveal the distribution of MMc cells in the whole embryo

No GFP signals were obtained from the transparent embryo

Mice fetuses were made successfully transparent even though the liver remained reddish. After making a whole embryo transparent by CUBIC system, I have analyzed the processed samples by light sheet microscope to identify GFP positive MMc cells. Around 600 images were obtained for each sample.

As can be seen in Fig 7, positive control sample for GFP (panel e), which is expressing GFP systemically, showed strong signals especially in muscular tissue, such as heart. On

the other hand, some organs such as liver showed rather weaker fluorescent signal. Despite detailed investigation of images I obtained, I could not identify GFP and RedDot2 double positive signal (Fig 7 c,d), and it was difficult to distinguish the true positive signals from background signals, especially in the organs which were not transparent enough, such as liver. I also could not identify GFP signals in Fig 7 c by comparing against the negative control (Fig 7 a), even though the positive control panel shows the intensive GFP signals (Fig 7 e). Based on these results, we decided to detect GFP by amplifying its signal by immunostaining.

No suitable anti-GFP antibody were found

Before testing the efficiency of anti-GFP antibodies, I confirmed that the staining technical control, anti-NeuN antibody worked successfully (Fig 8 to 10). Then, based on the results obtained for three antibodies tested (3E6, 1E4, 9F9.F9, Fig 8-10 respectively), I found that 3E6 anti GFP monoclonal antibody (invitrogen) showed the highest signal to noise (S/N) ratio (Fig 8) than the other two antibodies, suggesting that 3E6 would be the most suitable antibody for staining GFP. However, when laser excitation/gain level was adjusted, 3E6 antibody did not seem to have significant enhancement of signal intensity compared to the GFP fluorescence itself, or even much lower S/N ratio (Fig 11). Similarly, anti GFP polyclonal antibody (Anti GFP living colors Full-Length A.v. Polyclonal Antibody rabbit, Takara Bio Clontech) failed to obtain enhanced signal when compared to the original GFP signal (Fig 12). These results indicate that the widely used antibodies were not suitable for my experimental system.

Low sequence similarity between GFP used in this research and widely used GFPs

To figure out the reason why any anti-GFP antibody did not work, I compared the GFP sequences of my experimental system C57BL/6-Tg(CAG-EGFP)C14-Y01-FM131Osb (hereafter referred to as OkabeEGFP) with several GFP sequences that are widely used (Table 3). According to the report in which developed the transgenic mouse line (32), they used pEGFP-C1 for EGFP induction and the EGFP sequence is from 616 to 1329 bp (according to addgene: https://www.addgene.org/browse/sequence_vdb/2487/). Then, I extracted 720 bp of cording region of the EGFP sequence. This sequence and other five EGFP sequences were translated into amino acid sequences by Expasy, followed by calculating the similarity between these amino acid sequences by Needle (version 6.6.0).

As a result, I found that OkabeEGFP has unexpectedly lower similarity with other enhanced green fluorescent protein (EGFP) sequences at amino acid level (98.0% on average comparing to 99.3% on average of the similarity between other five EGFP sequences as shown in Table 4). Therefore, although the average difference was only 1.3%, it is possible that epitope(s) of purchased anti-GFP antibodies did not match with OkabeEGFP, leading to failure of signal amplification by immunostaining.

2.4 Discussion

2.4.1 Successful development of MMc cell isolation method

In this part, I successfully developed live MMc cell isolation method, and this method was suitable for embryonic stage E12.5 to E15.5 in mice. However, this method still has room for improvement, especially for isolating all MMc cells from a whole embryo in a truly comprehensive manner. First, possible bias would occur to the repertoire of cells since some cell types may have higher survival rate during the experimental procedure compared to others. For example, hepatocytes and cholangiocytes are reported to be fragile and sensitive to flow sorting, while cells such as endothelial cells are more robust (37). Secondly, as the tissue develops, it becomes more difficult to process the whole body. In order to isolate cells from whole embryos at later stages, it would be preferred to use stronger enzymes or extended reaction time, but this may cause severe damage to the cells, and the gene expression pattern could change drastically from the state in the body. Therefore, it is still challenging to observe the gene expression of the cells from later stages with the current technology.

2.4.2 Small difference in the amino acid sequences of GFP interfered with successful immunostaining of GFP.

While the embryo transparency itself worked well, except for some organs such as the liver, we failed to find GFP^+ maternal cells either by GFP fluorescence itself or even its amplification by immunostaining. To overcome this situation, it would be necessary to

produce or find antibodies specifically against the GFP used in our transgenic mouse for 3D cell distribution analysis. Furthermore, as a method to distinguish noise from real signals, establishment of detecting sparsely distributed GFP-positive cells would be necessary in the future study. In addition, unlike gels, actual embryos contain tissues of various hardness and shapes, which may pose additional unexpected challenges.

2.5 Figures and Tables

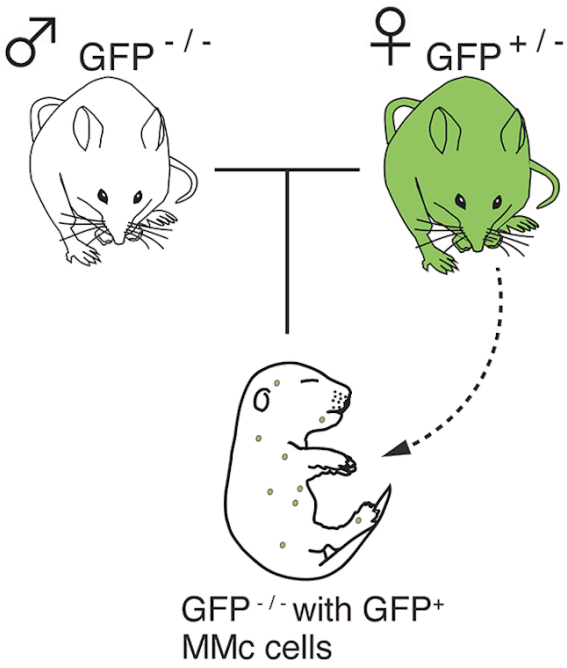

Fig. 1 Experimental design for detecting MMc cells in a fetus. Female mice heterozygous for the GFP locus ($GFP^{+/-}$) were mated with non-GFP-carrying wild-type male mice, and offspring with no GFP gene ($GFP^{-/-}$) were analyzed for $GFP^{+/-}$ MMc cells. (This figure is quoted from (38))

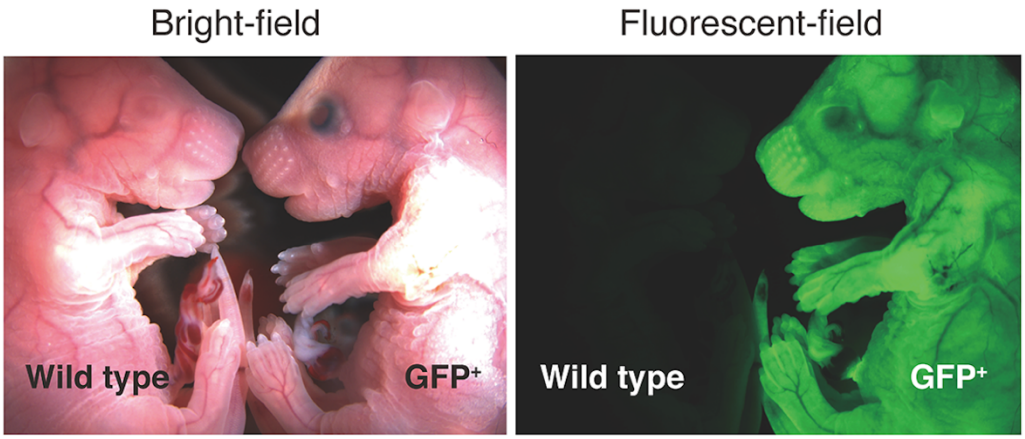

Fig. 2 A wild type fetus and a GFP expressing fetus from GFP positive mother. Bright-field and fluorescent-field images showed which fetus inherited the GFP gene (right) and which did not (E18.5, litter). $GFP^{-/-}$ fetus was used for MMc cell isolation. (This figure is quoted from (38))

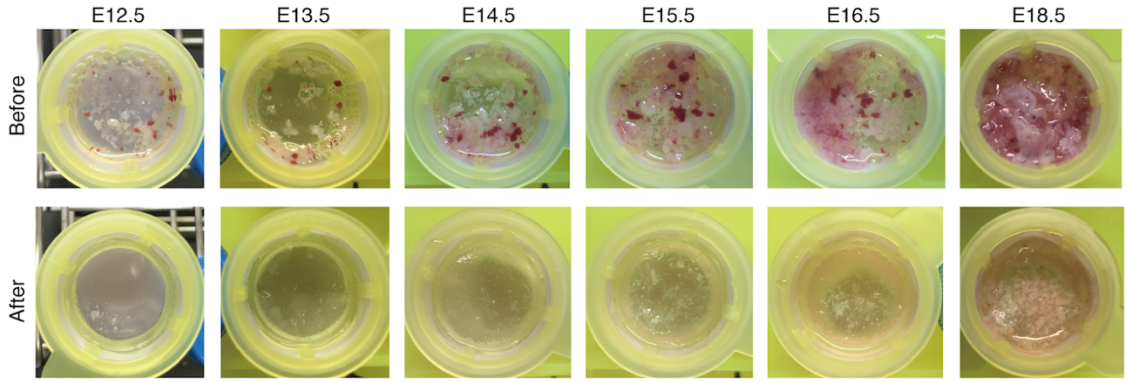

Fig. 3 Minced samples before and after the rough filtration are shown for each developmental stage. A 100-μm cell strainer was used for the rough filtration. Note that more aggregates remained in samples from the later stages E16.5 and E18.5. (This figure is quoted from (38))

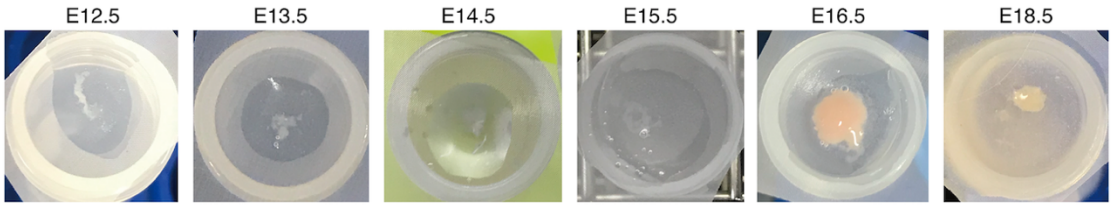

Fig. 4 Samples after fine filtration with the 70-μm cell strainer. Note that more aggregates remained in samples from the later stages E16.5 and E18.5. (This figure is quoted from (38))

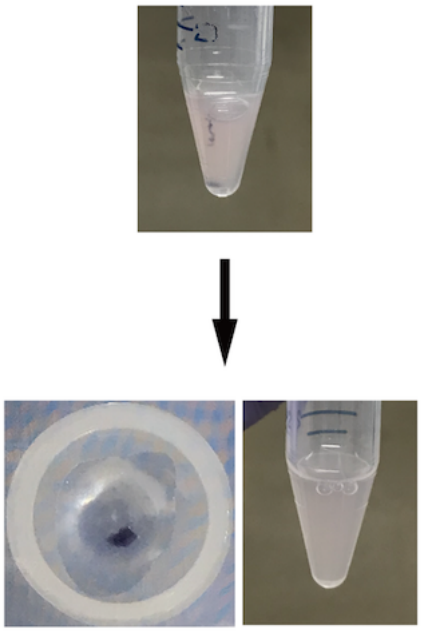

Fig. 5 The pre-filtered sample staining with trypan blue. Rough filtered samples were stained with trypan blue, and finer filtration was performed to estimate whether the aggregates were mainly composed of dead cells. (This figure is quoted from (38))

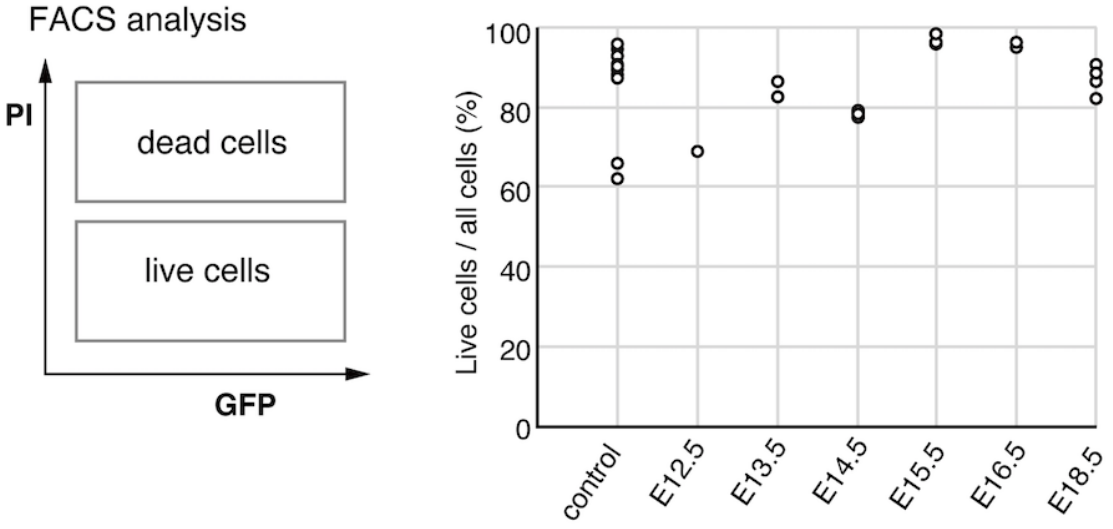

Fig. 6 Live cell rate in each developmental stage after the filtration process. Calculation of live cell rate (%) in the cell suspensions was evaluated using PI marker (dead cell marker) and FACS. The control sample originated from an adult spleen. Each circle represents the ratio of live cells in a single sample. [control: n = 11, E12.5: n = 1 (68.8%), E13.5: n = 2 (median 84.3%), E14.5: n = 5 (median 78.4%), E15.5: n = 4 (median 97.0%), E16.5: n = 2 (median 95.4%), E18.5: n = 4 (median 87.0%)]. (This figure is quoted from (38))

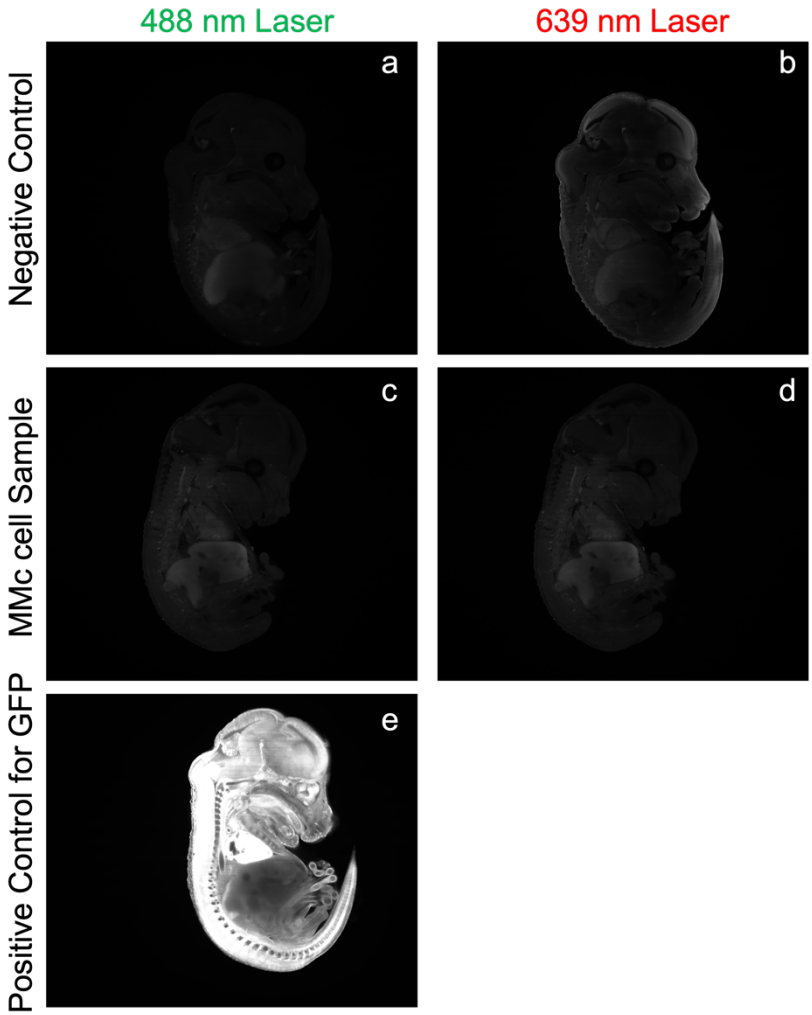

Fig. 7 Observation of the transparent whole mice embryos under light sheet microscope. 488 nm wave length and 639 nm were used for the detection of GFP positive cells in the embryos, and cell nuclei, respectively. A wild type embryo from wild type mother was set as negative control for GFP signal (panel a and b), and fetus with wild type phenotype from GFP positive mother was utilized as MMc cell sample (panel c and d), expected GFP positive MMc cells in the whole body. Systematically GFP expressing embryo was used as positive control for GFP signal (panel e). Images obtained in this experiment were processed by ImageJ.

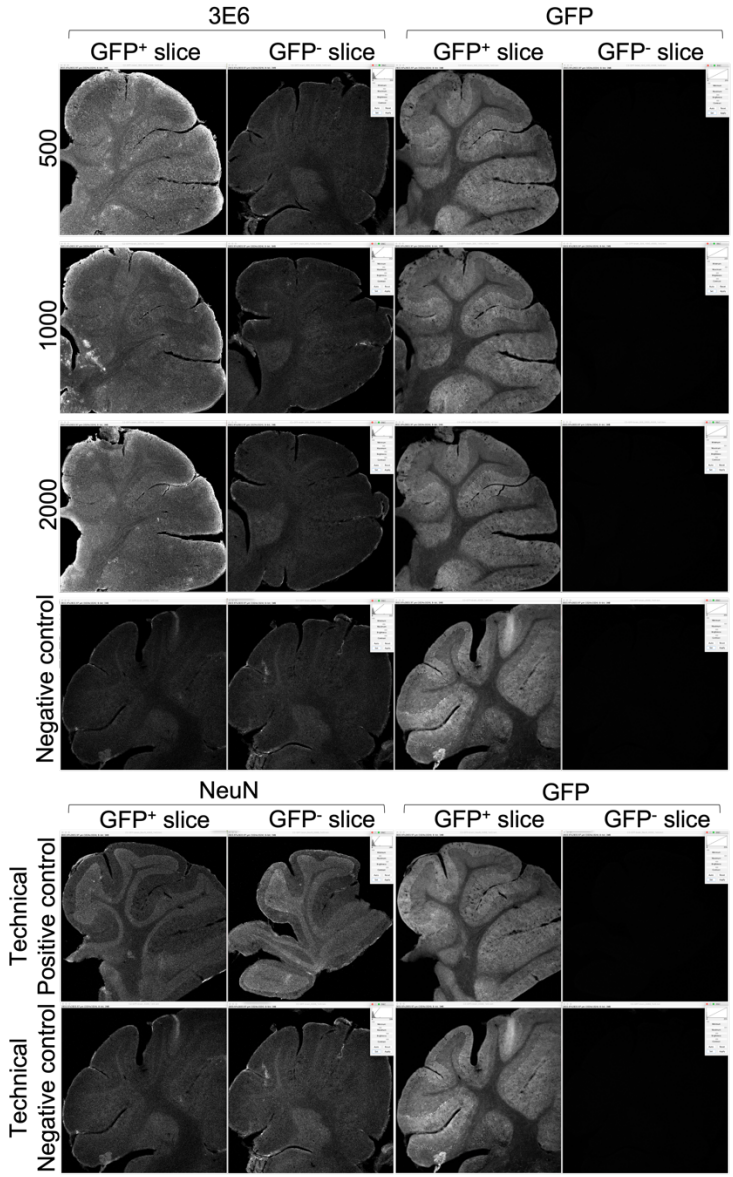

Fig. 8 Immunostaining of GFP with anti-GFP monoclonal antibody (3E6) mouse IgG2a (invitrogen). GFP expressing sections (GFP$^+$ slice) and WT sections (GFP$^-$ slice) from adult mice cerebellum were used for this experiment. Antibody 3E6 was diluted in 1:500, 1:1000, and 1:2000 as shown in the left side label of the pictures. Negative control and technical negative control were made by staining only with the secondary antibody but without primary antibody. On the other hand, technical positive control means sections with primary antibody. 2 columns of left side show the results of staining and the 2 columns of right side shows the GFP expression from these tissue themselves. Small boxes in the right corner are showing the values of Brightness/Contrast [100 for NeuN stained sections, 152 for each anti-GFP antibody stained sections, and 255 for GFP expressed by the tissue itself]. As the staining technical control, anti-NeuN antibody were used, and results indicate the antibody worked successfully.

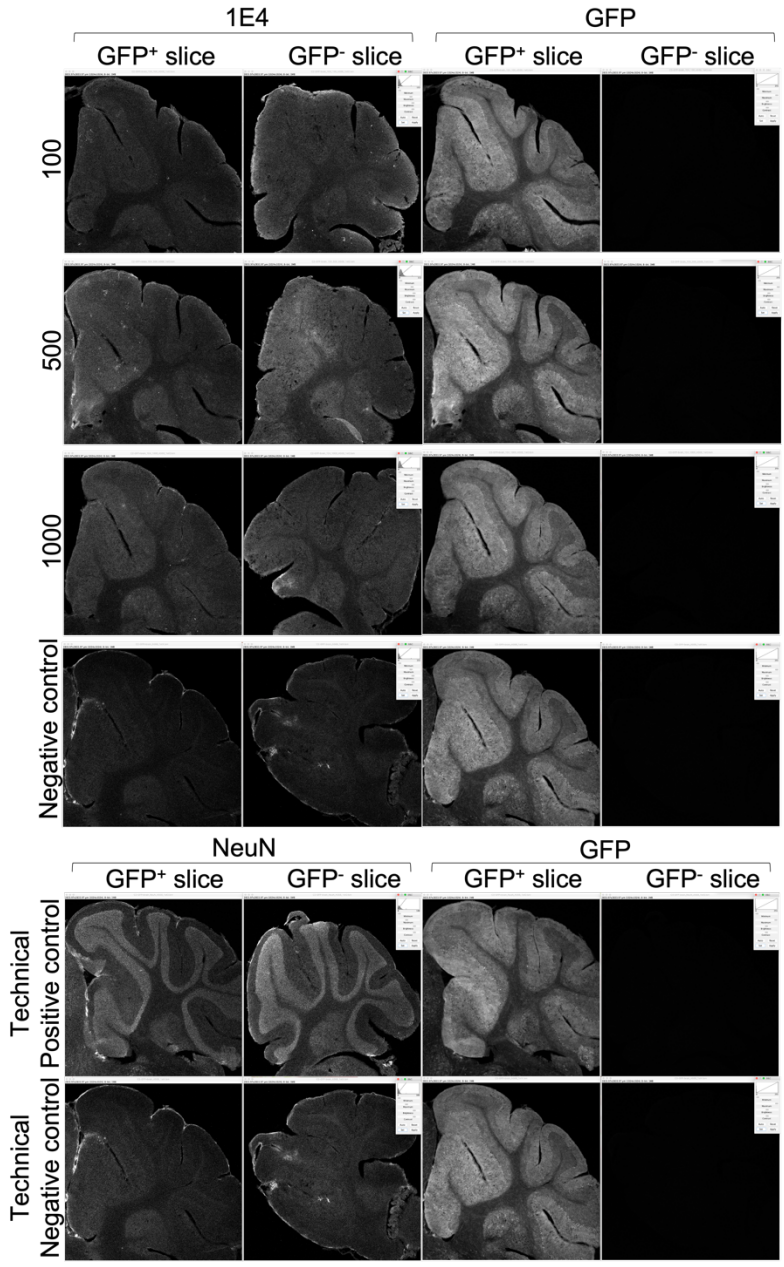

Fig. 9 Immunostaining of GFP with Anti-GFP mAb (M048-3, 1E4) mouse IgG2b (MBL). GFP expressing sections and WT sections from adult mice cerebellum were used for this experiment. Antibody 1E4 was diluted in 1:100, 1:500, and 1:1000 as shown in the left side label of the pictures. Negative control and technical negative control were made by staining only with the secondary antibody but without primary antibody. On the other hand, technical positive control means sections with primary antibody. 2 columns of left side show the results of staining and the 2 columns of right side shows the GFP expression from these tissue themselves. Small boxes in the right corner are showing the values of Brightness/Contrast [100 for NeuN stained sections, 152 for each anti-GFP antibody stained sections, and 255 for GFP expressed by the tissue itself]. As the staining technical control, anti-NeuN antibody worked successfully.

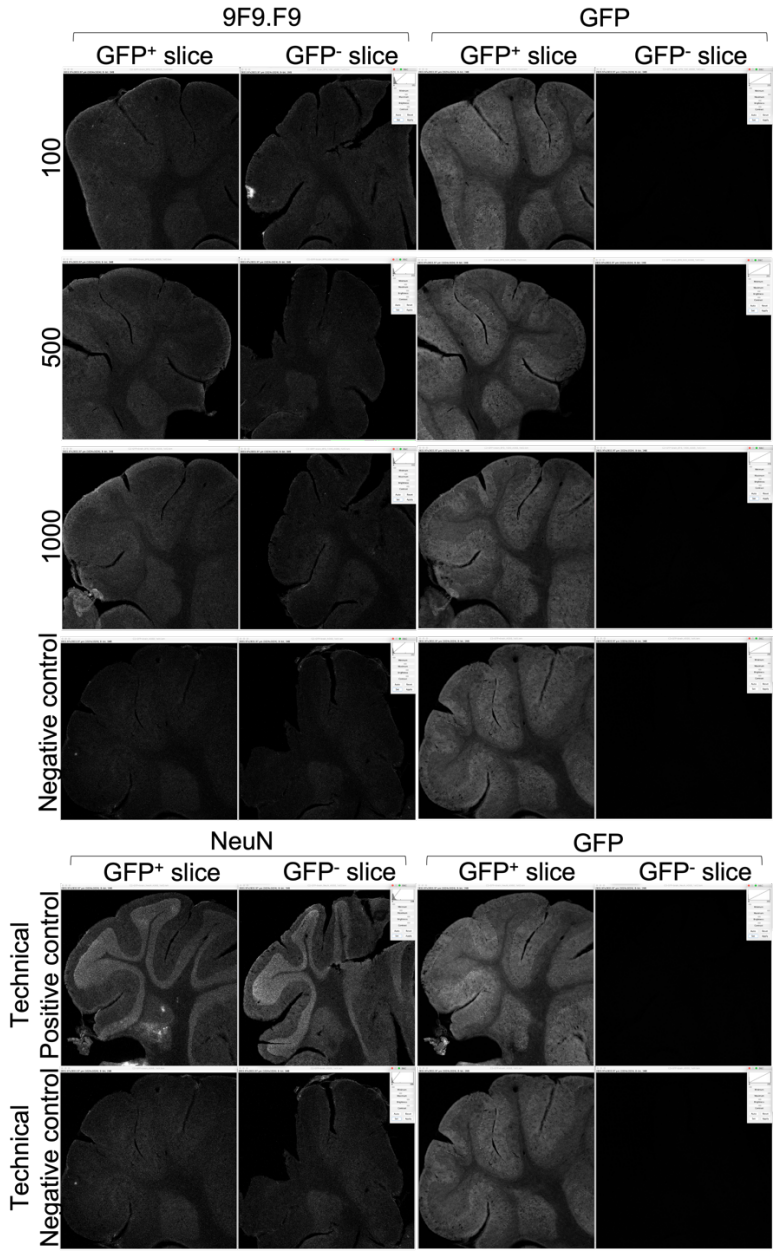

Fig. 10 Immunostaining of GFP with Anti-GFP antibody [9F9.F9] ab1218 (Abcam). GFP expressing sections and WT sections from adult mice cerebellum were used for this experiment. Antibody 9F9.F9 was diluted in 1:100, 1:500, and 1:1000 as shown in the left side label of the pictures. Negative control and technical negative control were made by staining only with the secondary antibody but without primary antibody. On the other hand, technical positive control means sections with primary antibody. 2 columns of left side show the results of staining and the 2 columns of right side shows the GFP expression from these tissue themselves. Small boxes in the right corner are showing the values of Brightness/Contrast [100 for NeuN stained sections, 152 for each anti-GFP antibody stained sections, and 255 for GFP expressed by the tissue itself]. As the staining technical control, anti-NeuN antibody worked successfully.

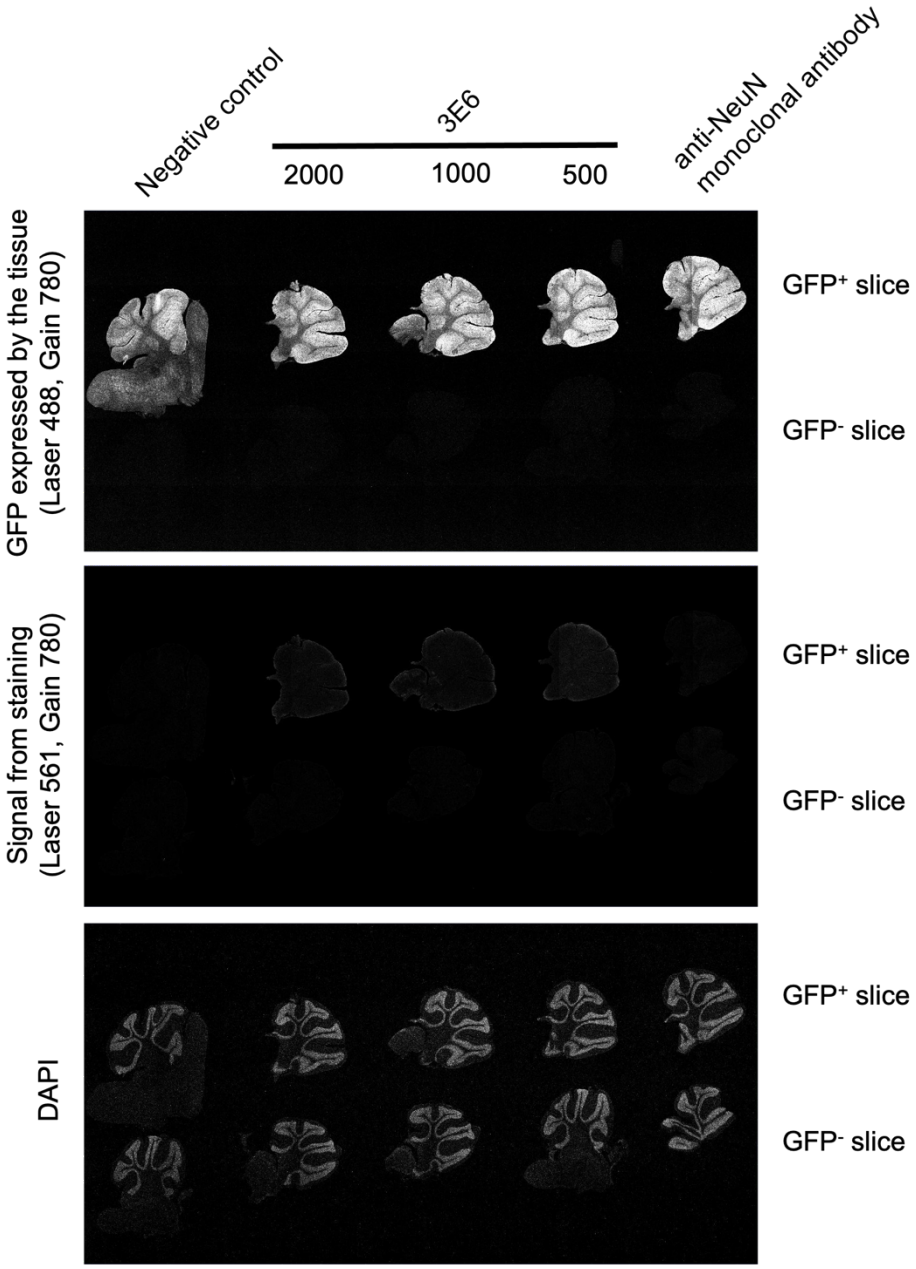

Fig. 11 Comparison of signal intensity between the tissue expressing GFP and the immuno-stained signals. These sections are the same sections as in Fig. 8. As shown on the top label, three concentration conditions of 3E6 antibody were prepared and taken pictures by fluorescence confocal microscopy (Zeiss LSM710), with excitation power 10.0 and emission gain was set to 780nm for both 488nm and 561nm excitation wave lengths. Negative control was made by staining only with the secondary antibody but without primary antibody. As the staining technical control, anti-NeuN antibody was used and it worked successfully as shown in Fig. 8.

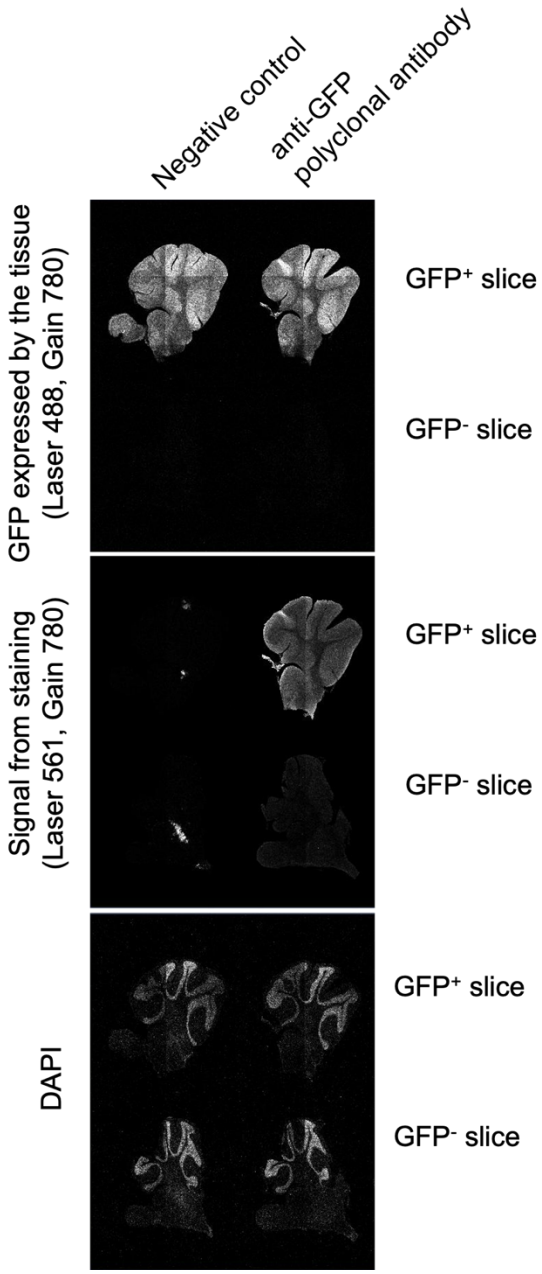

Fig. 12 Comparison of signal intensity between the tissue expressing GFP and the immuno-stained signals. This is the result of immunostaining with Anti GFP (living colors Full-Length A.v. Polyclonal Antibody) rabbit (Takara Bio Clontech). These pictures were taken by fluorescence confocal microscopy (Zeiss LSM710), with excitation power 10.0 and emission gain was set at 780nm for both 488nm and 561nm excitation wave lengths. Negative control was made by staining only with the secondary antibody but without primary antibody.

Table 1 List of antibodies used for choosing the most suitable antibody for revealing MMc cell distribution in a whole mouse embryo.

Product name	Company name	Lot number
GFP monoclonal antibody (3E6) mouse IgG2a	Invitrogen	2121763
Anti-GFP antibody [9F9.F9] ab1218	Abcam	GR213436-56
Anti-GFP mAb (M048-3, 1E4) mouse IgG2b	MBL	066
Anti GFP (living colors Full-Length A.v. Polyclonal Antibody) rabbit	Takara Bio Clontech	632592
Mouse Monoclonal Anti-NeuN Antibody (MAB377) IgG	Merck Millipore	3421975

Table 2 List of secondary antibodies.

Product name	Company name	Lot number
Alexa 555 goat anti mouse IgG, A21422	Mol Probes	751098
Goat anti-Mouse IgG (H+L) Highly Cross-Absorbed Secondary Antibody, Alexa Fluor 568, A11031	Thermo Fisher	2124366

Table 3 List of EGFP sequences.

>EGFP.AAA27721.1	ATGAGTAAAGGAGAAGAACTTTTCACTGGAGTTGTCC CAATTCTTGTTGAATTAGATGGTGATGTTAATGGGCA CAAATTTTCTGTCAGTGGAGAGGGTGAAGGTGATGCA ACATACGGAAAACTTACCCTTAAATTTATTTGCACTAC TGGAAAACTACCTGTTCCATGGCCAACACTTGTCACTA CTTTCTCTTATGGTGTTCAATGCTTTTCAAGATACCCA GATCATATGAAACAGCATGACTTTTTCAAGAGTGCCAT GCCCGAAGGTTATGTACAGGAAAGAACTATATTTTTC AAAGATGACGGGAACTACAAGACACGTGCTGAAGTCA AGTTTGAAGGTGATACCCTTGTTAATAGAATCGAGTT AAAAGGTATTGATTTTAAAGAAGATGGAAACATTCTT GGACACAAATTGGAATACAACTATAACTCACACAATGT ATACATCATGGCAGACAAACAAAAGAATGGAATCAAAG TTAACTTCAAAATTAGACACAACATTGAAGATGGAAGC GTTCAACTAGCAGACCATTATCAACAAAATACTCCAAT TGGCGATGGCCCTGTCCTTTTACCAGACAACCATTAC CTGTCCACACAATCTGCCCTTTCGAAAGATCCCAACGA AAAGAGAGACCACATGGTCCTTCTTGAGTTTGTAACA GCTGCTGGGATTACACATGGCATGGATGAACTATACA AATAA
>EGFP.AAA27722.1	ATGAGTAAAGGAGAAGAACTTTTCACTGGAGTTGTCC CAATTCTTGTTGAATTAGATGGTGATGTTAATGGGCA CAAATTCTCTGTCAGTGGAGAGGGTGAAGGTGATGCA ACATACGGAAAACTTACCCTTAAATTTATTTGCACTAC TGGAAAGCTACCTGTTCCATGGCCAACACTTGTCACT ACTTTCTCTTATGGTGTTCAATGCTTTTCAAGATACCC AGATCATATGAAACAGCATGACTTTTTCAAGAGTGCCA TGCCCGAAGGTTATGTACAGGAAAGAACTATATTTTA CAAAGATGACGGGAACTACAAATCACGTGCTGAAGTC AAGTTTGAAGGTGATACCCTCGTTAATAGAATTGAGT TAAAAGGTATTGATTTTAAAGAAGATGGAAACATTCTT GGACACAAAATGGAATACAACTATAACTCACACAATGT ATACATCATGGCAGACAAACAAAAGAATGGAATCAAAG TTAACTTCAAAATTAGACACAACATTGAAGATGGAAGC GTTCAACTAGCAGACCATTATCAACAAAATACTCCAAT TGGCGATGGCCCTGTCCTTTTACCAGACAACCATTAC CTGTCCACACAATCTGCCCTTTCCAAAGATCCCAACGA AAAGAGAGATCACATGATCCTTCTTGAGTTTGTAACA GCTGCTGGGATTACACATGGCATGGATGAACTATACA AATAA
>EGFP.AAA58246.1	ATGAGTAAAGGAGAAGAACTTTTCACTGGAGTTGTCC CAATTCTTGTTGAATTAGATGGCGATGTTAATGGGCA

	AAAATTCTCTGTCAGTGGAGAGGGTGAAGGTGATGCA ACATACGGAAAACTTACCCTTAAATTTATTTGCACTAC TGGGAAGCTACCTGTTCCATGGCCAACACTTGTCACT ACTTTCTCTTATGGTGTTCAATGCTTTTCAAGATACCC AGATCATATGAAACAGCATGACTTTTTCAAGAGTGCCA TGCCCGAAGGTTATGTACAGGAAAGAACTATATTTTA CAAAGATGACGGGAACTACAAGACACGTGCTGAAGTC AAGTTTGAAGGTGATACCCTTGTTAATAGAATCGAGT TAAAAGGTATTGATTTTAAAGAAGATGGAAACATTCTT GGACACAAAATGGAATACAACTATAACTCACATAATGT ATACATCATGGCAGACAAACCAAAGAATGGAATCAAAG TTAACTTCAAAATTAGACACAACATTAAAGATGGAAGC GTTCAATTAGCAGACCATTATCAACAAAATACTCCAAT TGGCGATGGCCCTGTCCTTTTACCAGACAACCATTAC CTGTCCACACAATCTGCCCTTTCCAAAGATCCCAACGA AAAGAGAGATCACATGATCCTTCTTGAGTTTGTAACA GCTGCTGGGATTACACATGGCATGGATGAACTATACA AATAA
>EGFP.CAA65278.1	ATGGGTAAGGGAGAGGAACTTTTCACTGGAGTTGTCC CAATCTTGGTTGAGCTCGACGGTGACGTCAATGGACA CAAGTTTTCCGTCTCAGGAGAGGGTGAAGGTGATGCA ACCTACGGAAAGTTGACCCTTAAGTTCATCTGCACTAC TGGAAAACTCCCTGTTCCTTGGCCAACATTGGTGACC ACTTTCTCTTACGGTGTTCAATGCTTCTCACGTTACCC AGACCATATGAAGCGTCATGACTTTTTCAAGTCCGCC ATGCCCGAGGGTTATGTGCAAGAGCGTACTATCTTCT TCAAGGACGACGGAAACTACAAGACACGTGCCGAAGT CAAGTTCGAAGGTGACACCTTGGTGAACAGAATCGAG TTGAAGGGTATCGATTTCAAGGAGGACGGAAACATTC TTGGACACAAGCTTGAGTACAACTACAACTCACACAAT GTGTACATCATGGCTGACAAGCAGAAGAACGGAATCA AGGTTAACTTCAAAATCCGTCACAACATTGAGGATGG AAGCGTTCAGTTGGCTGATCACTACCAACAGAATACT CCAATTGGCGATGGCCCTGTGCTTTTGCCAGACAACC ACTACTTGTCCACCCAATCTGCCCTTTCCAAAGATCCC AACGAAAAGAGAGACCACATGGTCTTGCTTGAGTTTG TGACCGCTGCTGGCATTACCCACGGCATGGATGAGTT GTACAAGTAA
>EGFP.AAB18957.1	ATGTCTAAAGGTGAAGAATTATTCACTGGTGTTGTCC CAATTTTGGTTGAATTAGATGGTGATGTTAATGGTCA CAAATTTTCTGTCTCCGGTGAAGGTGAAGGTGATGCT ACTTACGGTAAATTGACCTTAAAATTTATTTGTACTAC TGGTAAATTGCCAGTTCCATGGCCAACCTTAGTCACT

	ACTTTCGGTTATGGTGTTCAATGTTTTGCTAGATACC CAGATCATATGAAACAACATGACTTTTTCAAGTCTGCC ATGCCAGAAGGTTATGTTCAAGAAAGAACTATTTTTTT CAAAGATGACGGTAACTACAAGACCAGAGCTGAAGTC AAGTTTGAAGGTGATACCTTAGTTAATAGAATCGAAT TAAAAGGTATTGATTTTAAAGAAGATGGTAACATTTTA GGTCACAAATTGGAATACAACTATAACTCTCACAATGT TTACATCATGGCTGACAAACAAAAGAATGGTATCAAAG TTAACTTCAAAATTAGACACAACATTGAAGATGGTTCT GTTCAATTAGCTGACCATTATCAACAAAATACTCCAAT TGGTGATGGTCCAGTCTTGTTACCAGACAACCATTAC TTATCCACTCAATCTGCCTTATCCAAAGATCCAAACGA AAAGAGAGACCACATGGTCTTGTTAGAATTTGTTACT GCTGCTGGTATTACCCATGGTATGGATGAATTGTACA AATAA
>OkabeEGFP	ATGGTGAGCAAGGGCGAGGAGCTGTTCACCGGGGTG GTGCCCATCCTGGTCGAGCTGGACGGCGACGTAAACG GCCACAAGTTCAGCGTGTCCGGCGAGGGCGAGGGCG ATGCCACCTACGGCAAGCTGACCCTGAAGTTCATCTG CACCACCGGCAAGCTGCCCGTGCCCTGGCCCACCCTC GTGACCACCCTGACCTACGGCGTGCAGTGCTTCAGCC GCTACCCCGACCACATGAAGCAGCACGACTTCTTCAA GTCCGCCATGCCCGAAGGCTACGTCCAGGAGCGCACC ATCTTCTTCAAGGACGACGGCAACTACAAGACCCGCG CCGAGGTGAAGTTCGAGGGCGACACCCTGGTGAACCG CATCGAGCTGAAGGGCATCGACTTCAAGGAGGACGGC AACATCCTGGGGCACAAGCTGGAGTACAACTACAACA GCCACAACGTCTATATCATGGCCGACAAGCAGAAGAA CGGCATCAAGGTGAACTTCAAGATCCGCCACAACATC GAGGACGGCAGCGTGCAGCTCGCCGACCACTACCAGC AGAACACCCCCATCGGCGACGGCCCCGTGCTGCTGCC CGACAACCACTACCTGAGCACCCAGTCCGCCCTGAGC AAAGACCCCAACGAGAAGCGCGATCACATGGTCCTGC TGGAGTTCGTGACCGCCGCCGGGATCACTCTCGGCAT GGACGAGCTGTACAAGTCC

Table 4 Results of similarity calculation of GFP sequences by Needle.

EGFP .AAB18957.1	EGFP .CAA65278.1	EGFP .AAA58246.1	EGFP .AAA27722.1	EGFP. AAA27721.1	Okabe EGFP	
						Okabe EGFP
					98.3%	EGFP. AAA27721.1
				100.0%	98.3%	EGFP. AAA27722.1
			99.2%	99.2%	97.5%	EGFP. AAA58246.1
		98.7%	99.6%	99.6%	97.9%	EGFP. CAA65278.1
	99.2%	98.7%	99.6%	99.6%	97.9%	EGFP. AAB18957.1

The average percentage of sequence similarity between OkabeEGFP and other EGFP sequences was 98.0%. On the other hand, the average % of sequence similarity between other five EGFP amino acid sequences was 99.3%.

Chapter 3　Isolation of MMc cells from whole-embryonic mice samples and comparison of its numbers

3.1 Introduction

As discussed in Chapter 1, previous studies have implied that MMc cells are reported to be involved in various phenomena in both beneficial and harmful ways, such as establishment and maintenance of immunological tolerance, tissue repair, and on the other hand, pathogenesis or deterioration of some inflammatory diseases, based on the findings that MMc cells were enriched in various phenomena. However, there is no direct evidence showing MMc cells can cause these symptoms. Therefore, I hypothesized if there are differences in the number and cell-type repertoire of MMc cells among individual embryos, which could lead to seemingly inconsistent phenomena (immunological tolerance, tissue repair, and inflammatory disease). Because previous studies only focused on the specific tissue or phenomena for searching the frequency or number of MMc cells, it is still unknown whether the number of MMc cells in the whole healthy embryo differs among individuals or not. Moreover, no study so far has analyzed the overall composition of MMc cell population, although some cell types were revealed as MMc cells by using cell type specific markers. Consequently, to answer my hypothesis, counting and isolating MMc cells are essential points. By utilizing the MMc isolation method I have developed, I will show the number of MMc cells in a whole mouse fetus and discuss the difference between individuals in this Chapter, and isolate MMc cell as single cells for Chapter 4.

3.2 Material and Methods

Mouse strains

As explained in Chapter 2, I used the same mice lines of GFP, and mating strategy to create GFP heterozygous female mouse and wild type fetus, which are supposed to include GFP positive maternal cells.

Preparation of cell suspensions from whole embryo

To obtain suspensions of dissociated cells from the whole embryo, GFP^- embryos (identified by the absence of fluorescence using GFP excitation flashlight while embryos are in amnion) were carefully dissected from their sacrificed mother to avoid cross-contamination of fetal and maternal cells. Then, the embryos were processed with the established method in Chapter 2, and single cell suspensions were obtained one embryo each.

To create positive control for MMc cells, blood of the sacrificed mother was collected. For these maternal blood cells, erythrocyte removal was conducted twice because the amount of red blood cells are much more abundant than fetus samples but has no nuclei. First round removal was performed with the same method done for the fetus samples, and in the second round with ACK treatment for 3 min. The embryos from the same developmental stage as sample embryos were used as negative control.

MMc cell counting and observation

The cells (> 10,000,000 cells, which roughly corresponds to one-fourth of total cell suspension volume) obtained from a single fetus were stained with Propidium Iodide (PI)

solution and were loaded into a fluorescence-activated cell sorting (FACS) machine (BD AriaIIIu). After removing doublet cells and separating the live cell and dead cell populations by PI marker, the number of GFP positive live cells (GFP^+ PI^- cells) was counted as the number of MMc cells (Fig 13). The frequency of MMc cells was calculated and normalized to the number of MMc cells per 10,000,000 fetal (GFP^- PI^-) cells. Sorted MMc cells were transferred into a glass-bottom dish and observed by fluorescence confocal microscopy (Zeiss LSM710) to check positive signal for the GFP and negative signal for the PI.

3.3 Results

Possible differences in frequency of MMc cells among individual fetuses.

After obtaining the cell suspension from a single mouse embryo using the filtering method described in Chapter 2, I further processed these cells by FACS to identify and count live MMc cells. I first removed dead and doublet cells using PI staining and gating. As shown in Fig 14, noise signals and/or debris were removed with gate P1, and then doublet cells were removed with gates P2 and P3. P4 gate setting for the GFP^+ PI^- (live MMc cells) was performed by checking the signal intensity of positive control cells (cells from maternal blood). Around 1×10^7 cells were loaded into the FACS, and the GFP^+ PI^- cells were counted. Finally, the frequency of MMc cells was calculated as the number of MMc cells over 10^7 PI^- cells (Fig 15). Although some false positive signals were detected in the samples from E14.5 negative controls, the other stages detected no GFP^+ PI^- cells in the negative control samples (cells prepared from a wild-type embryo with a wild-type mother). In contrast, many $GFP^{-/-}$ embryos with $GFP^{+/-}$ mothers contained GFP^+ cells. GFP signals of these potential maternal cells in the $GFP^{-/-}$ embryos were also confirmed using microscopy (Fig 16). These results indicate that maternal cells were successfully detected using this method in a single embryo. Meanwhile, GFP^+ cells were not detected in some of the $GFP^{-/-}$ embryos. Given that all embryos are considered to have maternal cells (13), the results suggest that my method is not sensitive enough to detect MMc cells in some of the embryos. Additionally, given the false positive signals in the negative control samples, it is also possible that some false positive signals were contained in the tested samples. Nevertheless,

the frequencies of GFP^+ signals in the tested samples were higher than those in the negative control samples, and one sample from stage E18.5, showed as high as 1800 cells over 10^7 cells. Together, these results suggest that this method detects MMc cells to a higher level than negative control samples. It is also worth noting that the frequency of maternal cells may differ largely in some rare cases, as for the stage E18.5 embryo.

3.4 Discussion

In this Chapter, I counted the number of MMc cells from a whole mouse embryo by using the developed method in Chapter 2. The purpose of this study was to test if the number of maternal cells differed among individual embryos. Although I could not completely exclude the false positive signals from contaminated maternal cells during the experimental procedure, the overall signals were higher in the test samples than in the negative control samples (Fig 15). Of note, I found that majority of the embryos showed a comparable number of MMc cells, around 3.7 cells / 10^7 sorted cells for those detected with GFP^+ cells (Fig 15, Table 5). Meanwhile, an unexpected finding was that one of the embryos at the latest stage (E18.5) showed 1,816 cells/10^7 cells, which corresponds to a frequency approximately 500 times higher than that in the detected embryos (average 3.7 cells/ 10^7). I suspected a possible contamination of mother blood cells during the sample preparation process for this sample; however, considering that the sample preparation protocol comprises multiple careful washing steps and that no GFP^+ cells were detected in the vast majority of the negative controls. To add, another possibility was that the GFP^+ cells identified here could be from $GFP^{+/-}$ siblings in the same liter, however, considering that the litter with the sample had relatively lower ratio of $GFP^{+/-}$ siblings compared to those of the other stages (the ratio of $GFP^{+/-}$: $GFP^{-/-}$ embryos of the E18.5 was 0.23:1 in the sample litter, where it was 1:1.2 on average in the litters of the other stages. See also Table 5), and I also avoided using embryos with conjugated placenta, the probability of this sibling origin scenario appears to be less likely. Even a minor possibility would be that the embryo was a

tetragametic chimera, leading to the high frequency of GFP^+ cells, however, at least I could not find any sign of abnormality, including body size, morphology, and patchy signals of GFP. Thus, it would be fair to conclude that most of the cells detected here were MMc cells or at least immunologically non-self cells. Finally, considering that later stages are known to show higher frequency of MMc cells (36), it is intriguing that the sample with highly frequent MMc cells was detected for the latest embryonic stage. Consistently, while no significant correlation was obtained between the number of MMc cells and developmental stages, however, I still found a weak tendency even without stage 18.5 (Spearman's correlation coefficiency 0.3 for stages from 12.5 to 16.5). Together, these results suggest that while most of the embryos have a comparable number of MMc cells, a much higher count can be detected in some rare cases. Given this finding, it is intriguing to know if these high-MMc embryos are associated with a variety of MMc-related phenomena that appear to be contradictory to each other (6)(7)(19)(20)(21)(22)(23)(24)(25)(26)(27)(28)(29). With this respect, it is tempting to know the mechanism behind the variations in the number of MMc^+ embryos among the litters (e.g., Litter C vs D, Litter H and I in Table 5). Finally, major caveats of this methodology would be that 7 – 8 hours are needed to process embryos to obtain single celled suspension and is not best suited to the mouse embryos from the latest stages (Fig 3,4). This, together with automatically removed cells in FACS as an electronic aborts (around 1 in 100 counts in my experiments) may explain the reason why we could not detect GFP^+ cells in some of the embryos. Furthermore, while this experimental design cannot exclude the possibility of detecting GFP^+ cells from $GFP^{+/-}$ siblings in the same litter, this could be solved by crossing mother having GFP^+/ Red

fluorescent protein (RFP)$^{+}$ on the same locus, with non fluorescent wild type male. In this design, GFP/RFP double positive cells in either GFP$^{+/-}$ or RFP$^{+/-}$ fetus should always be the cells of maternal origin.

3.5 Figures and Tables

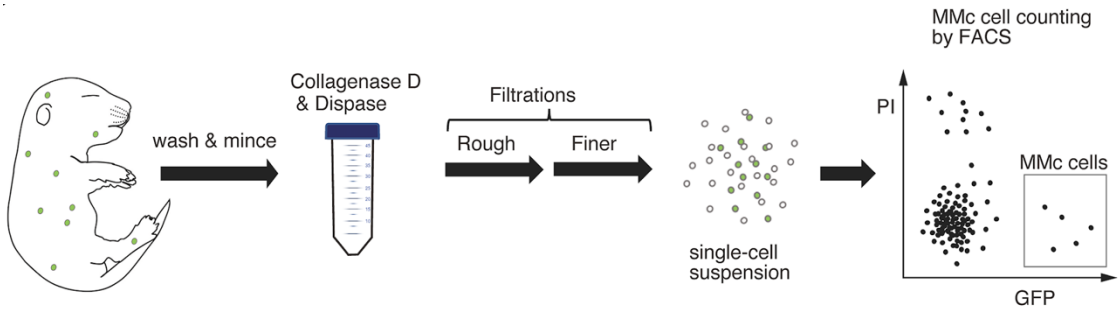

Fig. 13 Schematic illustration of the developed method for detecting MMc cells from a whole embryo (see also Method). To avoid cross-contamination of maternal cells, an isolated embryo was washed three times in cold phosphate-buffered saline. The embryo was then minced and incubated in an enzyme cocktail, followed by two (rough and fine) filtrations to dissociate cells. Rough filtration was carried out to dissociate the solid tissues, followed by fine filtration to generate a single cell suspension. From this single cell suspension, live MMc cells were counted and isolated using FACS. (This figure is quoted from (38))

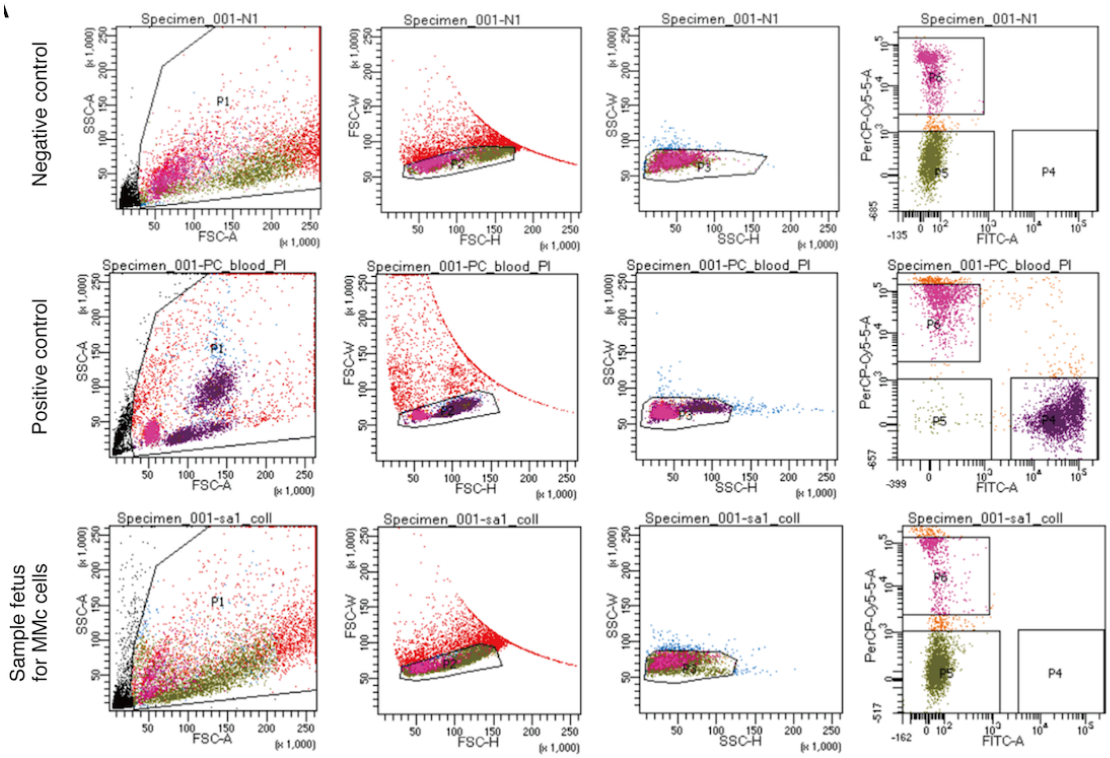

Fig. 14 FACS gating conditions for counting MMc cells. After the rough and finer filtration of the minced embryo, isolated cells from a single $GFP^{-/-}$ embryo were analyzed using FACS. Mother blood cells were used as positive control, and cells from a wild-type fetus with a wild-type mother were used as negative control. Noise and/or debris were removed with gate P1, and then doublet cells were removed with gate P2 and P3. Gate P4 (GFP^{+} PI^{-}) was defined using positive control cells and applied to sort the GFP^{+}, potential MMc cells. (This figure is quoted from (38))

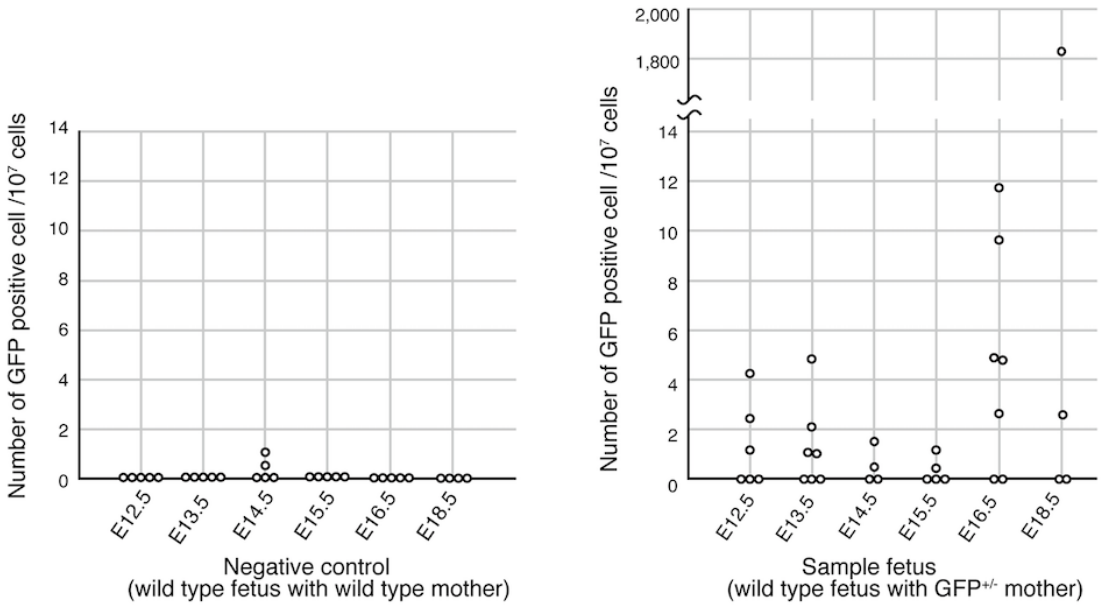

Fig. 15 The frequency of MMc cells in fetuses. For each sample (individual embryo), the numbers of sorted MMc cells were counted as GFP^+ cells, and the ratios over the 10^7 sorted cells were calculated. Some GFP^+ cells were detected for the negative control samples (wild-type embryo with wild-type mother). Sample numbers are as follows. control: E12.5: n = 5, E13.5: n = 5, E14.5: n = 5, E15.5: n = 5, E16.5: n = 5, E18.5: n = 4, sample: E12.5: n = 6, E13.5: n = 7, E14.5: n = 4, E15.5: n = 5, E16.5: n = 7, E18.5: n = 4. See also Table 4 for more detail. (This figure is quoted from (38))

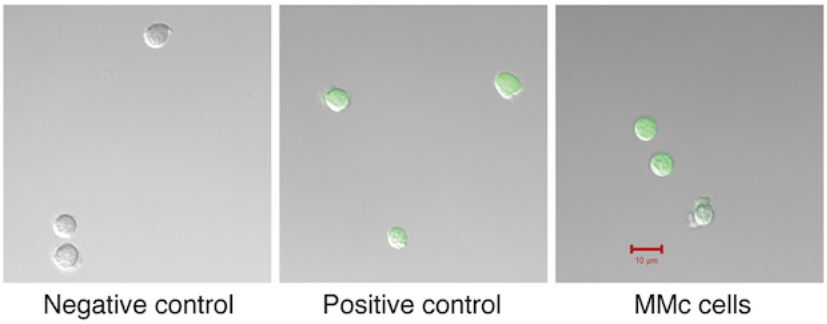

Fig. 16 GFP signals of sorted cells were further analyzed using fluorescent confocal microscopy (Zeiss LSM710). Together with the sample cells, negative (wild-type cells sorted with gate P5) and positive control (mother blood cells sorted with gate P4) cells were also analyzed using microscopy. (This figure is quoted from (38))

Table 5 Detailed information of GFP+ and GFP- fetal samples in Fig. 15 (This table is quoted from (38))

stages	litters	# of total embryos	# of GFP+ and GFP- embryos	GFP- fetus	# of detected GFP+ cells	# of total sorted cells (processed events count)	Frequency of GFP+ cells (/10^7)
E12.5	Litter A	11	7 : 4	A_a	0	14845653	0
				A_b	0	15583576	0
				A_c	3	12591640	2
				A_d	5	11957752	4
	Litter B	4	2 : 2	B_a	0	15130672	0
				B_b	2	17418976	1
E13.5	Litter C	10	6 : 4	C_a	4	8363224	5
				C_b	0	19424512	0
				C_c	0	13583552	0
				C_d	0	11746550	0
	Litter D	12	4 : 8	D_a	1	9638845	1
				D_b	2	20525153	1
				D_c	3	14678961	2
E14.5	Litter E	9	4 : 5	E_a	2	13667524	1
				E_b	1	21182691	0
	Litter F	10	8 : 2	F_a	0	17686309	0
				F_b	0	15668245	0
E15.5	Litter G	11	4 : 7	G_a	2	17827792	1
				G_b	1	23348680	0
				G_c	0	18040216	0
				G_d	0	33750160	0
				G_e	0	20301805	0
E16.5	Litter H	14	5 : 9	H_a	8	8409021	10
				H_b	5	19457597	3
				H_c	10	20648028	5
				H_d	10	21205760	5
				H_e	19	16388294	12
	Litter I	2	0 : 2	I_a	0	16528251	0
				I_b	0	21958902	0
E18.5	Litter J	9	2 : 7	J_a	5	19551458	3
				J_b	0	24253026	0
				J_c	0	14541005	0
				J_d	2686	14786949	1816

Chapter 4　MMc cell type estimation by utilizing single cell RNA-seq

4.1 Introduction

Previous studies reported that various cell types have been observed as MMc cells in various situations. However, no research showed the whole picture of MMc cell population. In other words, we still do not know which cell types are included as MMc cells in our bodies and how much of certain cell types consists of the major proportion of MMc population.

Generally, immunostaining the cell surface marker protein has been used for cell type definition. This relies largely on proteins expressed on cell surface, and require specific antibodies, implying that many cell types could have been overlooked. To overcome this technical limitation, I adopted single cell RNA-seq and combined it with my developed MMc cell isolation method to estimate MMc cell type more comprehensively from the gene expression pattern of each cell.

4.2 Material and Methods

Mouse strains

With the same mouse lines and mating strategies as shown in Chapter 2, I obtained GFP heterozygous female mice and wild type fetuses (E14.5) from GFP heterozygous female mice. The fetuses' father has homozygous H-2Kd, shown as d/d in Fig. 17, as its MHC gene. On the other hand, the fetuses' mother has H-2Kd and H-2Kb, shown as d/b in Fig. 17 as its major histocompatibility complex (MHC) gene because this female mouse was born of wild type mother, which has BALB/c background with H-2Kd, and the mother was mated with GFP homozygous father, which has C57BL/6 background with H-2Kb. When the GFP heterozygous female mouse was mated with wild type BALB/c male mouse, her fetuses have d/b or d/d as their MHC genes.

Tissue dissociation

Single cell suspensions of fetuses (E14.5), which are holding MMc cells as GFP positive cells, were obtained with same protocol as one in Chapter 3. The cell concentration was calculated for each cell suspension and used for adjusting the volume of MACS in the next step.

To create positive and negative controls for MMc cells and for the gate setting, blood of the sacrificed mother and wild type mice were collected. As shown in Chapter 3, for these blood cells, erythrocyte removal was conducted twice because the amount of red blood cells are much more abundant than fetus samples. First round removal was performed with the same method done for the fetus samples, and in the second round with ACK treatment for 3 min.

MMc cell enrichment by Magnetic-Activated Cell Sorting (MACS)

Before loading the single cell suspensions onto FACS, MMc cells were enriched by Magnetic-Activated Cell Sorting (MACS, Miltenyi Biotec K.K.). In MACS, the target cells will be enriched through magnetic stand by staining a specific cell surface marker by fluorescent dye and magnetic beads. Since I used two different backgrounds of mice, GFP heterozygous mother mice have H-2Kb protein as MHC on its cell surface. Although there is a one in two chance of the fetuses have H-2Kb protein, it is still possible for the other half of fetuses to separate the maternal cells by its cell surface marker.

To enrich MMc cells by MACS, the single cell suspensions from fetuses were stained by APC conjugated anti-mouse H-2Kb antibody, followed by beads reaction by adding anti-APC beads. These beads conjugated cell samples were ran through the magnetic column and the target cells were washed out after all samples were ran. The detailed protocol is below.

After the cell concentration calculation, cell suspension samples were centrifuged at 300×g for 10 min at 4℃. After removing the supernatant, the supernatant of hybridoma 2.4G2 was added as Fc receptor blocker, then incubated for 10 min at 4℃. APC anti-mouse H-2Kb antibody (clone AF6-88.5, BioLegend, Cat# 116518) was diluted into 1:80 as the final concentration with MACS buffer [D-PBS, 0.2% (v/v) BSA] and added into FcR blocked cell samples, then the cell suspensions were incubated for 30 min at 4℃ under darken situation. To wash out the extra antibody, FACS buffer [HBSS(-), 0.5% BSA, 2mM EDTA] was added to the cell suspensions and centrifuged at 1,300 r.p.m. for 6 min at 4℃. Next, as beads reaction, anti-APC MicroBeads (Miltenyi Biotec K.K., Order no. 130-090-855) was added to the cell suspensions (cell : beads = 4×10^7 cells : 80 μl), followed by mixing with

pipetting and incubating for 15 min at 4°C under darken situation. Then, MACS buffer [D-PBS, 0.2% (v/v) BSA] was added to wash out the extra beads, followed by centrifugation at 1,300 r.p.m. for 6 min at 4°C. After removing the supernatant, 500 μl of MACS buffer [D-PBS, 0.2% (v/v) BSA] was added into the cell suspensions, and this cell samples were loaded onto the magnetic column (MS Column, Miltenyi Biotec K.K., Order no. 130-042-201), which was set on the magnetic field (OctoMACS Separator, Miltenyi Biotec K.K., Order no. 130-042-109), by through 70 μm filter. This column was equalized with 500 μl of MACS buffer [D-PBS, 0.2% (v/v) BSA] before the sample loading. The sample loaded columns were then washed 3 times with 500 μl MACS buffer [D-PBS, 0.2% (v/v) BSA]. After washing, the columns were separated from the magnetic field and 1 ml MACS buffer was loaded on the column, followed by pushing out the target cells with syringe, then positive fractions including target cells were collected. All collected cell fractions were centrifuged at 1,300 r.p.m. for 6 min at 4°C, followed by removing supernatant and by adding 100 μl MACS buffer [D-PBS, 0.2% (v/v) BSA] for the positive fractions and 200 μl for the negative fractions.

Maternal blood cells were stained with the same antibody used for fetal cells; APC conjugated anti-mouse H-2Kb antibody (clone AF6-88.5, BioLegend, Cat# 116518) to confirm the staining condition and to set selection gates for MMc cell isolation. Staining protocol of the blood cells was also same as fetal cell staining; GFP positive cells with and without staining, and GFP negative cells with and without staining. For the cells without staining, I added the same volume of MACS buffer [D-PBS, 0.2% (v/v) BSA] instead of antibody liquid. After washing of the extra antibody and centrifugation at same condition as

fetal cells, 100 μl MACS buffer [D-PBS, 0.2% (v/v) BSA] was added.

MMc cell isolation by FACS

Before loading cell samples onto FACS (BD AriaIIIu), all cell samples were stained with Propidium Iodide (PI) solution to separate live cells from dead cells. With blood cell samples, the parameters for FACS, including the gate for the target cells, was set. In this experiment, MMc cells were isolated as $PI^{-}GFP^{+}APC^{+}$ in the gate P9. MMc cells were collected by single cell sorting mode, and the cells were sorted into 96-well PCR plate with 3 μl of "the receiving solution". 10×Reaction Buffer was made with 10×Lysis Buffer containing 0.05% of RNase Inhibitor (both regents are from SMART-Seq v4 Ultra Low Input RNA Kit for Sequencing, Clontech, 634890). Receiving solution was made by mixing 0.5 μl of 10×Reaction Buffer and 2.5 μl of RNase-free water. Collected cells were centrifuged and kept in -80℃ until the sequencing procedures.

Single cell RNA-seq

For single cell RNA-seq of MMc cells, Smart-seq2 (39) protocol was adopted, as it is advantageous for detecting the low frequency of cells and has low loss ratio.

First-strand cDNA synthesis: In this process, all steps were conducted under Open clean workstation. I used SMART-Seq v4 Ultra Low Input RNA Kit for Sequencing (Clontech, 634890) by following the User Manual with some modifications. In brief, for priming and template switching at the 5' end of the transcript, 3' SMART-Seq CDS Primer II A and SMART-Seq v4 Oligonucleotide are used. As the technical positive control, I used control total RNA associated with the kit instead of that from collected cells. The control

total RNA (1 μg/μl in original concentration) was diluted into 4×10^{-6} μg/μl, used 3 μl to roughly match with the RNA amount of a single cell (0.1 pg). For technical negative control, RNase-free water was used instead of total RNA or a cell. In addition, 1 μl of ERCC as spike-in control was also added to all the samples and controls, diluting into about 10386 molecules/μl. After mixing the all required reagents, samples were primed at 72℃ for 3 min, followed by reverse transcription (42℃ for 90 min, 70℃ for 10 min, and 4℃ forever).

cDNA amplification by LD-PCR: By following the User Manual of SMART-Seq v4 Ultra Low Input RNA Kit for Sequencing, I conducted all procedures under Open clean workstation. In this step, PCR primer II A amplifies cDNA from the sequences introduced by 3' SMART-Seq CDS Primer II A and SMART-Seq v4 Oligonucleotides. After mixing all reagents needed, cDNA amplification was conducted with the following PCR condition; 95℃ for 1 min, 22 cycles of 98℃ for 10 sec, 65℃ for 30 sec and 68℃ for 3 min, and lastly 72℃ for 10 min.

Purification of amplified cDNA and quality check by Qubit and Bioanalyzer: By following the User Manual of SMART-Seq v4 Ultra Low Input RNA Kit for Sequencing, the amplified samples were purified with Agencourt AMPure XP and 80% ethanol. After purification, concentrations of double strand DNA of each sample were calculated by Qubit with Qubit dsDNA HS Assay Kit (Invitrogen, Cat. No. Q32851). To confirm that cDNA was properly amplified, the purified samples were analyzed with Bioanalyzer. The volumes of each sample were calculated as to be 1ng/μl from the results of Qubit measurement. For Bioanalyzer measurements, I used Agilent High Sensitivity DNA Kit

(#5067-4626) and chose dsDNA High Sensitivity DNA as Assays.

Tagmentation: Tagmentation was done by using Nextera XT Library Prep Kit (96 samples, illumine, FC-131-1096) and Nextera XT index Kit v2 set A (96 indexes 384 samples, illumine, FC-131-2001). In this process, I followed Nextera XT DNA Library Prep Reference Guide with some modifications. In brief, the input DNA concentration was estimated as 1 ng in 5 μl from the results of Qubit measurements, followed by tagementation of genomic DNA, library amplification, and cleaning up of libraries. After the cleaning, quality was evaluated by the concentration and amplified library having 250 – 1,000 bp length DNA using Qubit and Bioanalyzer, respectively. The same quality evaluation was also done for the samples after the cDNA amplification.

Sequencing by NovaSeq6000: Before multiplexing all samples, each sample was prepared as 500 μl of 10 nM multiplex library, and added appropriate amount of libraries into a tube. This multiplexed library was sequenced by NovaSeq6000 (Flow cell type: SP, 150 bp pair end).

RNA-seq data analysis for cell type estimation

First, quality of the single cell RNA-seq fastq files were verified by FastQC (v0.11.9), followed by adapter trimming by Trimmomatic. Clean fastq files were then mapped to the mouse genome (Mus_musculus.GRCm39.dna_rm.toplevel.fa) with EGFP sequence (extracted from EGFP sequence of pEGFP-C1 (addgene), which was used in the development of this Tg line (32)) added, using HISAT2 (2.2.1). This sequence will be referred to as OkabeEGFP. Then, relative gene expression levels were estimated by

processing the mapped data with stringTie (v2.1.6) with EGFP sequence added GTF files (Mus_musculus.GRCm39.104.gff3). To estimate the cell types of isolated cells, Tabula Muris data which consists of massive single cell RNAseq data from 20 organs (40) was referred, as well as detected marker genes in each single-cell sample. Since this study targets only maternal cells, I used only data from female mice in Tabula Muris data (24,259 samples). Tabula Muris data was downloaded from AWS (s3://czbiohub-tabula-muris/facs_bam_files/) and transformed into fastq files by bam2fastq from samtools, then processed these fastq files as same as MMc cells' fastq files to create the gene expression matrix. Clustering of gene expression tables (made from potential maternal cells and Tabula Muris) were done by Seurat (ver 4.0.4). Only samples with 500 genes expressed (defined by Seurat with default options) were used. Each cell type of Tabula Muris was confirmed by referring annotations_facs.csv of Tabula Muris.

4.3 Results

62 isolated cells were all GFP positive and *SRY* negative.

Within sixteen GFP negative fetuses from stage E14.5 processed, two embryos had detectable numbers of live GFP^+ cells (2 cells from one embryo, and 61 cells from the other one) by the method I developed in Chapter 2 and 3. Although the original purpose of the study was to compare cell type repertoires between individual embryos, I modified the aim into revealing the cell type repertoire of MMc cell population of one embryo. After the quality checking process by Qubit and Bioanalyzer, one cell couldn't pass the check. 62 cells were sequenced by NovaSeq6000 (150 bp, paired end), followed by data analysis as shown in 4.2 of this Chapter. As a result, the average read depth of each sample was 6,520,827 reads per cell and the average number of detected (TPM > 0) gene was 8,059 genes per cell. In all the isolated cells, OkabeEGFP gene expression was detected, while no cells expressed *SRY* gene (ENSMUSG00000069036), indicating that these isolated cells were female origin. Although it is still possible that these cells contained those from female GFP positive siblings.

Determination of the 'dimensionality' of the data and performance of clustering.

By following the 'Seurat – Guided Clustering Tutorial' (compiled: August 30, 2021) linear dimensional reduction (principal component analysis; PCA) was performed to determine the 'dimensionality' of the Tabula Muris data set (which consists of single cell RNAseq data from 20 organs and 79 cell types, Table 6 and 7) before estimating the cell types by clustering analysis. In the dimensionality determination process, Elbow plot was adopted for this purpose. Elbow plot is a ranking of principle components based on the percentage of

variance explained by each one. As shown in Fig. 18, the Elbow plot showed that there are several 'elbows', suggesting that there is possibility that the majority of true signal is likely to be captured in the first to 2, 6, 11 or 20 principal components (PCs). Based on the result, I created UMAP of for these PC numbers (Fig. 19), and decided to utilize the 11 PCs and 20 PCs, as these had relatively higher clustering resolutions. To further identify which PC parameter (11 PCs and 20 PCs) is more suitable for the following analyses, I first confirmed that OkabeEGFP expressing cells, or MMc cells, were successfully clustered in multiple clusters for both of the PC conditions, suggesting that Tabula Muris can be utilized for cell type estimation of MMc cells (Fig 20, 21, Table 8, 9). In addition, I have also tested if the clustering results match well with the annotated cell types of Tabula Muris (annotations_facs.csv). For both of the PC conditions, I defined the cell type of each cluster by the highest number of cells (Table 10 and 11), and analyzed if each cluster had a unique cell type. In the 11 PCs condition, 3 cell types were clustered into multiple clusters (endothelial cell in cluster 2 and 10, epithelial cell of large intestine in cluster 9 and 13, and luminal epithelial cell of mammary gland in cluster 17 and 19). Similarly, 3 cell types were clustered into multiple clusters in the 20 PCs condition (endothelial cell in cluster 4, 15 and 24, immature T cell in cluster 7 and 19, and luminal epithelial cell of mammary gland in cluster 16 and 21). However, considering that the endothelial cell was clustered in three clusters, it would be reasonable to say that the 11 PCs condition performs better than the 20 PCs condition.

MMc cells types estimated by referring to Tabula Muris data

Under the condition of 11 PCs, MMc cells were clustered into the cluster 0, 5, 6, 8, 10, 11, 12, 18, 19, 22, and 25 (Table 8). To estimate their cell type, I first referred to the cell type of Tabula Muris cells in the same cluster, then checked if the marker, or representative genes of each cell type were expressed in MMc cells. For the cluster 0, where two MMc cells were classified, fibroblast and mesenchymal cell were the representative cell types. In both of the MMc cells, expression of *Pdgfrb*, which is the marker gene of mesenchymal cell, was observed. I also confirmed the expression of *Atxn1*, which also suggests that these cells are mesenchymal stem cell. Next, around 56% of isolated MMc cells were classified into the cluster 5 (Table 8), and its representative cell types were myeloid cell, leukocyte and macrophage based on Tabula Muris annotation file. Consistently, most of the MMc cells in cluster 5 expressed macrophage marker genes (*Selplg*$^{+}$, *Cd14*$^{+}$, *Cd3e*$^{-}$, *Cd19)*, and some expressed myeloid cell marker genes (*Itgam*$^{+}$, *Cd68*$^{+}$, *C1qa*$^{+}$, *Lyz2*$^{+}$, *Cd14*$^{+}$). The cluster 6 of Tabula Muris cells were annotated as immature T cell as the biggest population followed by natural killer cell, however, the single MMc cell identified in this cluster did not express the marker genes for both these cell types. Specifically, within four genes for immature T cell marker (*Cd3e*$^{+}$, *Cd4*$^{+}$, *Cd8a*$^{+}$, and *Cd6*$^{+}$) only showed expression of *Cd3e*$^{+}$ and *Cd4*$^{+}$, but lacked *Cd8*$^{-}$ and *Cd6*$^{-}$ expressions. Since MMc cells are reported to have tolerative effect for offsprings, I also searched for MMc cells expressing Foxp3, as this gene is known as a highly specific intracellular regulatory marker gene of regulatory T cell. While none of the MMc cells of cluster 6 showed Foxp3 expression, some MMc cells clustered in 5 and 10 showed expressed of *Foxp3* gene (more than 1 TPM). Intriguingly, some cells with macrophage cell markers also showed Foxp3 expression. One cell was clustered into cluster

8, which include basal cell of epidermis as the biggest population followed by keratinocyte stem cell. *Krt10* and *Sbsn* genes are known as the marker genes of epidermis, and I found that these two genes were both expressed in the MMc cell. For cluster 10 (annotated as endothelial cells by clustering analysis), while six MMc cells were classified all cells did not show the expression of the marker genes for endothelial cell (*Cdh5*$^{+}$, *Pecam1*$^{+}$, *Fabp4*$^{+}$, *Cav1*$^{+}$), and they only expressed *Fabp4* and *Cav1* but not *Cdh5* and *Pecam1*. In addition, I also checked the marker genes expression for endocardial cell (*Npr3*$^{+}$) and myofibroblast cell (*Myh11*$^{+}$, *Tcf21*$^{+}$), but combinations of both of genes were not observed in any of the MMc cells. For cluster 11 (annotated as astrocyte by the clustering analysis), two MMc cells were clustered and one of them actually showed the expression of astrocyte marker genes (*Aldh1l1*$^{+}$, *Slc1a3*$^{+}$, *Aqp4*$^{+}$). In the meanwhile, the other cell did not express the *Aldh1l1* gene but did the *Slca3* and *Aqp4*. For the cluster 12, skeletal muscle satellite cell (*Pax7*$^{+}$, *Pax3*$^{+}$, *Myod1*$^{+}$, *Myf5*$^{+}$) and mesenchymal cell (*Pdgfrb*$^{+}$) were the major representative cell types, however, none of the MMc cell in this cluster did not express any of these marker genes. In cluster 18, six MMc cells were sorted into this cluster and one of them showed the gene expression of proliferation marker (*Mki67*), and half of these six cells showed the myeloid cell markers (I*tgam*$^{+}$, *Cd68*$^{+}$, *C1qa*$^{+}$, *Lyz2*$^{+}$, *Cd14*$^{+}$) and the other half missed only the expression of *C1qa*. In cluster 19, two MMc cells were estimated as epithelial cell with the gene expression of *Krt14*$^{+}$, *Krt5*$^{+}$, *Krt17*$^{+}$. On the other hand, although the cluster 25 showed that epithelial cell of lung was the most sorted cell type, MMc cells in this cluster did not show the gene expression of the cell type. However, two cells of them showed low expression level of *Aire* (about 0.3 TPM), which is autoimmune regulator. Finally, one cell

sorted into cluster 22 showed the gene expression of hepatocyte (*Alb*$^{+}$, *Ttr*$^{+}$, *Apoa1*$^{+}$, *Serpina1c*$^{+}$).

Together, although some of MMc cell types were not clear, it can be said that most of the cell in MMc cell population are immune related cell types. Of note, some MMc cells were proliferating cells, stem cells and terminally differentiated cells (Fig. 22 and 23).

All MMc cells expressed genes of transmembrane proteins involved in migration.

To find a common feature of MMc cells, I extracted the genes expressing in all isolated MMc cells as TPM >10. As a result, I found 26 genes, commonly expressed in all of the MMc cells. Besides 18 of the constantly expressed genes, such as housekeeping genes, and 8 genes with unknown functions, two genes of membrane proteins involved in migration were extracted; lymphocyte antigen 6 complex, locus E (*Ly6e*) and interferon induced transmembrane protein 3 (*Ifitm3*).

4.4 Discussion

In many previous studies, researchers have focused on immune related cells rather than other cell types because MMc cells carry non-self antigens (especially non-inherited maternal antigen, or NIMA) for the fetus and it has been considered that MMc cells have immunological influences on child, such as immunological tolerance, and inflammatory disease. Consequently, no research elucidated the overall cell type repertoire of MMc cells. In this study, I successfully isolated and analyzed gene expression profiles of 62 *GFP* expressing MMc cell from 2 whole mouse embryos. From this result, I have estimated the cell types of each single MMc cells and found that around 66% of the population is occupied by immune related cell types. In addition, I found that there are 16% of terminally differentiated tissue specific cell types, such as hepatocyte, astrocyte and epidermis (Fig. 23). Moreover, around 5% of the MMc population expressed the genes of proliferating or mesenchymal stem cells. These results suggests that not only immune related cells, but also other cell types are included as MMc cells.

As has been reported that MMc cells are known to be observed in the later period of life (7), MMc cells were expected to include those with stem cell potential, and previous study has actually shown that this kind of stem cell related MMc cells exists in offspring (18). Consistently, I found that the possibility of mesenchymal stem cell existence in this study, suggesting that maternal mesenchymal stem cells migrate into fetus as early as E14.5. Although the ratio of proliferating or stem cells was only 5% in the present study, these cells could be one of the major ancestral cells which lasts until the rest of life, if they occupied

their stem cell niches.

To my surprise, not only stem cells, but also terminally differentiated tissue specific cell types were found in this study. It is still possible that these cells first migrated as undifferentiated cell type and then differentiated in the fetus after migration. However, considering that MMc cell migration starts as early as E12.5–E13.5 in mice (13)(14), and our sample is embryos of E14.5, it is likely that terminally differentiated cell, or near terminally differentiated cells migrated to the fetus as MMc cells. In any case, it is tempting to know if these differentiated MMc cells contributes to the peripheral tolerance for non-inherited maternal antigens, or priming the fetal immune system to attack the NIMA related antigens.

Furthermore, I have detected autoimmune regulator (*Aire*) gene expression in three cells with low level, and these cells showed the gene expression of medullary thymic epithelial cells (mTECs) (*Aire*$^{+}$, *Cldn3*$^{+}$, *Cldn4*$^{+}$ (41)), suggesting that not only the specific cell types' antigens, but also various of cell specific antigens would be presented to fetal cells by these MMc cells. If these *Aire* expressing MMc cells acquired their niche in the fetal mTECs, it is possible for MMc cells to continuously provide the tolerating induction against NIMA to the offspring immune system. This could be contributing to successful organ transplant between mother and fetus (42)(43) or stable pregnancy in the next generation (19). In addition, considering better prognosis is known for NIMA matched sibling transplantation than that of NIMA mismatched condition (21)(31), it is still possible that MMc cells are contributing to tolerance to NIMA. Consistently, one study utilizing mice experiment showed that mice with high levels of MMc cells showed low response to NIMA (44). Combining these

evidences and my results, it implies that the more MMc cells migrate, the chance that the fetus obtains tolerance to NIMA increases. Further, this could also be contributing to MMc cells to be retained in the fetus for a long time. In this study, I succeeded in identifying two gene coding membrane proteins involved in cell migration, as the genes expressed in all isolated MMc cells; *Ly6e* and *Lfitm3*. Of note, both of these genes are known to be involved in cell migration. Lymphocyte antigen 6 complex, locus E (*Ly6e*) is a member of the lymphostromal cell membrane Ly6 surperfamily protein. This gene expresses in a variety of malignant solid tumors (45), and overexpression of this gene is known to promote metastasis of gastric cancer (46). Interferon induced transmembrane protein 3 (*Ifitm3*) gene is expressed in migratory primordial germ cells and regulates cell adhesion and differentiation (47). It has been reported that overexpression of this gene promotes the metastasis of hepatocellular carcinoma (48). Although further experiments are required, it is possible that MMc cells utilize these cell migration related membrane proteins to migrate from mother to fetus, providing additional hints toward how MMc cells pass through the placental barrier. There are a few studies which studied the mechanism of MMc cell migration into fetus. C. Chen *et al.* showed that maternal multipotent mesenchymal stromal cells can migrate into fetus by utilizing vascular endothelial growth factor receptor-1 and integrins (49). Another previous study has shown that a chemokine (C-C motif) ligand 3 (CCL3) is not essential for the migration of maternal cells in mouse by using a chemokine (C-C motif) ligand 3 (CCL3)-deficient mouse model (50).

4.5 Figures and Tables

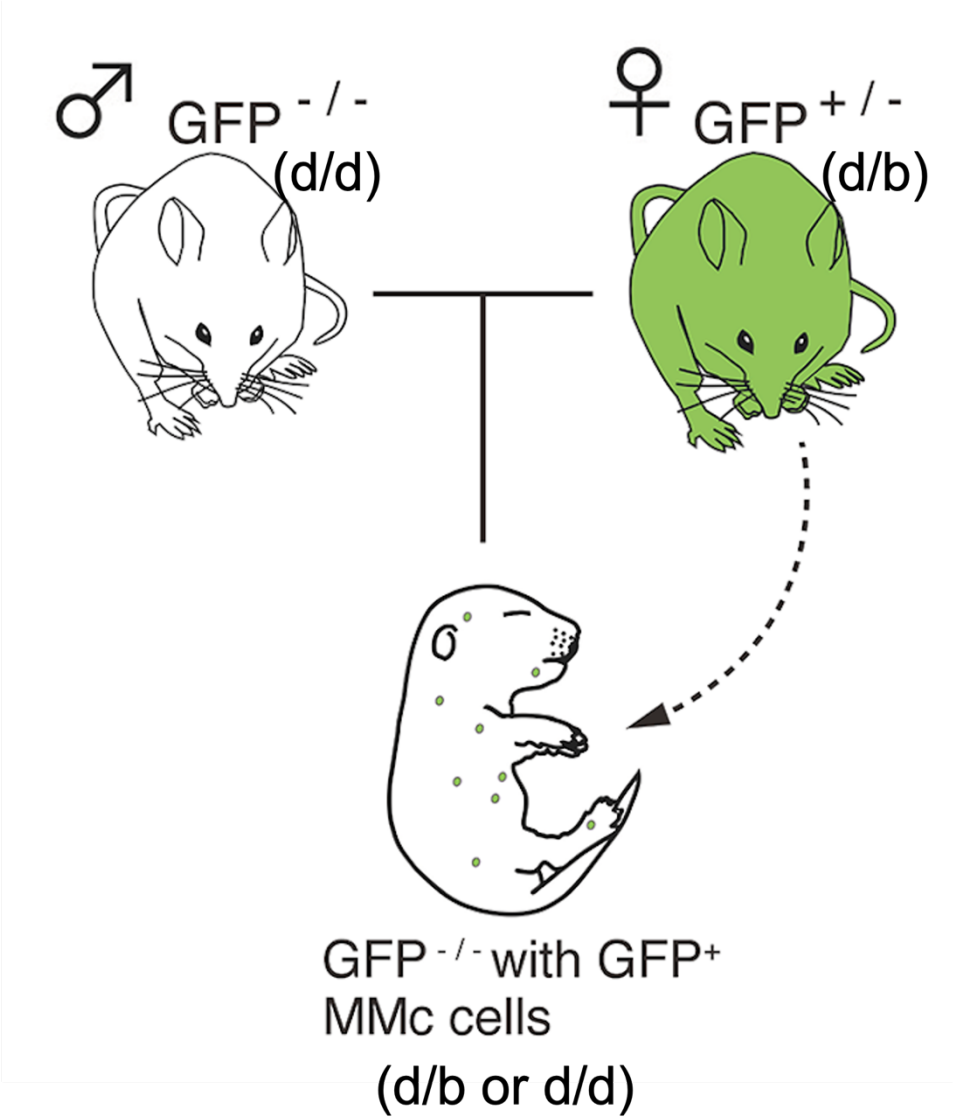

Fig. 17 Experimental design for detecting MMc cells. Father mice have homozygous H-2Kd, shown as d/d in this Fig (Fig. 1 modified), as its MHC gene. On the other hand, the mother mice have H-2Kd and H-2Kb, shown as d/b in this Figure. In this experimental system, maternal cells can be detected as $GFP^{+}H\text{-}2Kb^{+}$cell in the $GFP^{-/-}$ fetus.

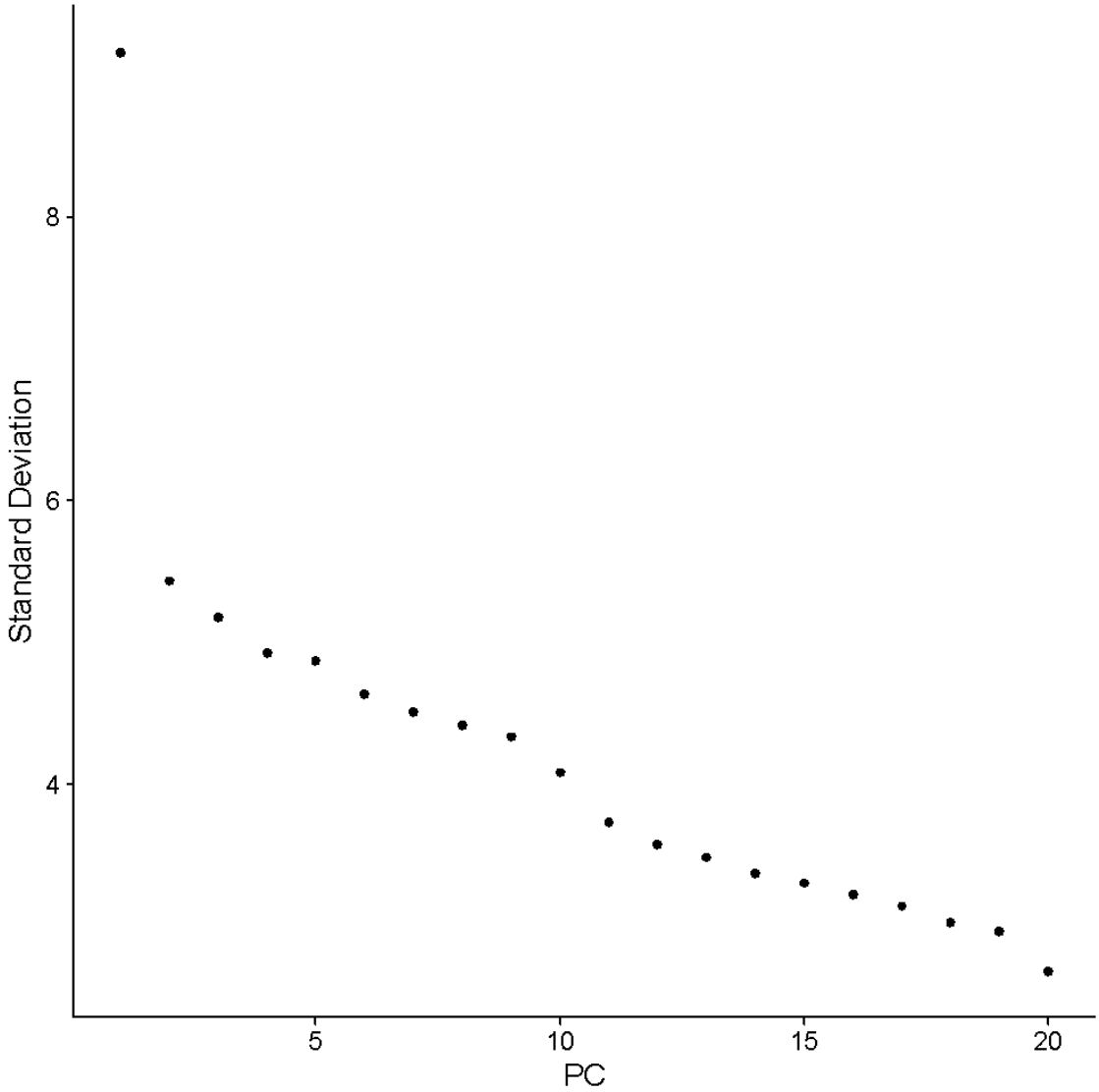

Fig. 18 Elbow plot of the gene expression matrix data which includes both data of Tabula Muris and isolated 62 MMc cells. Elbow plot is a ranking of principle components based on the percentage of variance explained by each one.

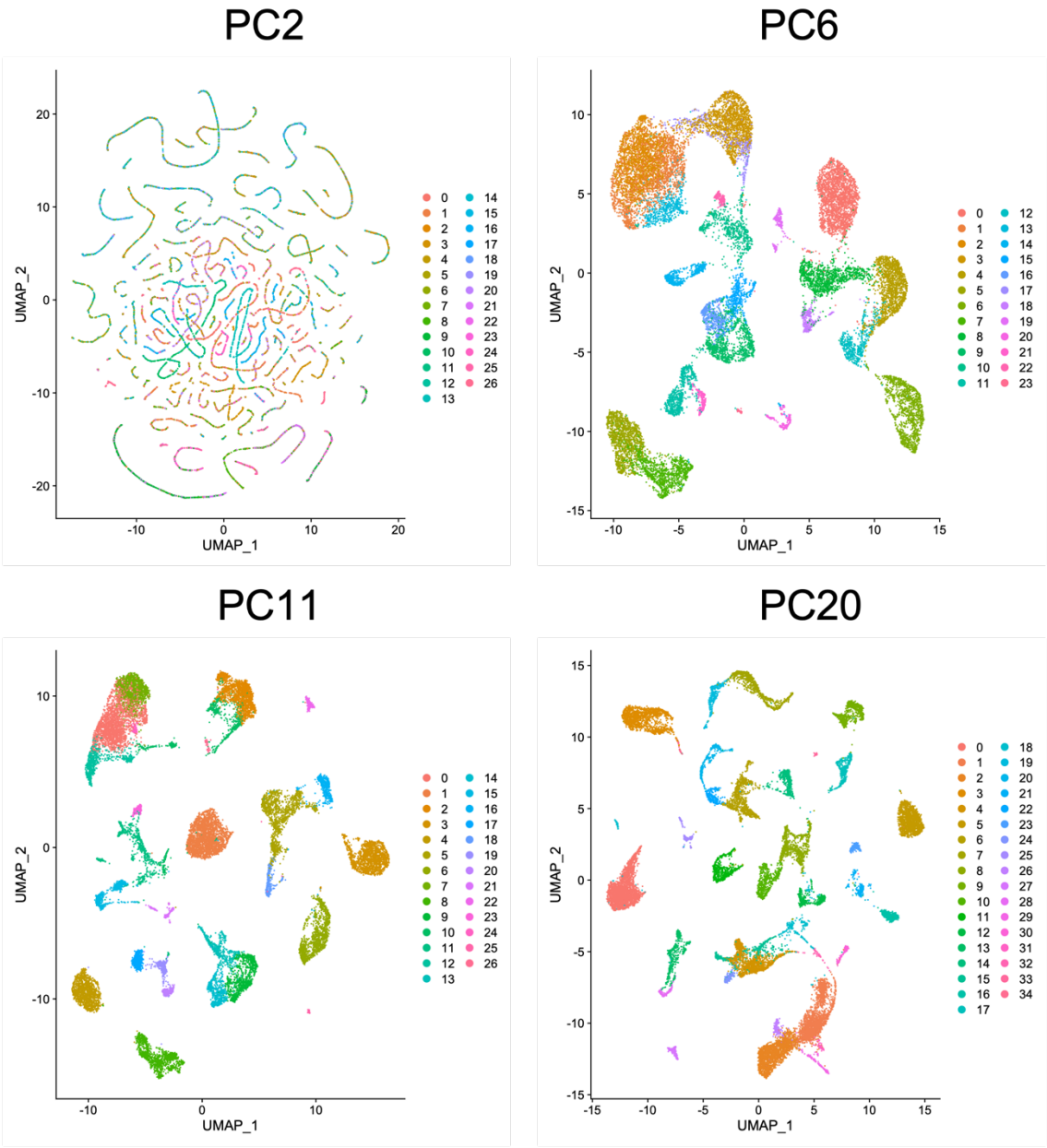

Fig. 19 Results of clustering by changing the number of PCs. These four PC values were picked up from the result of Elbow Plot in Figure 18.

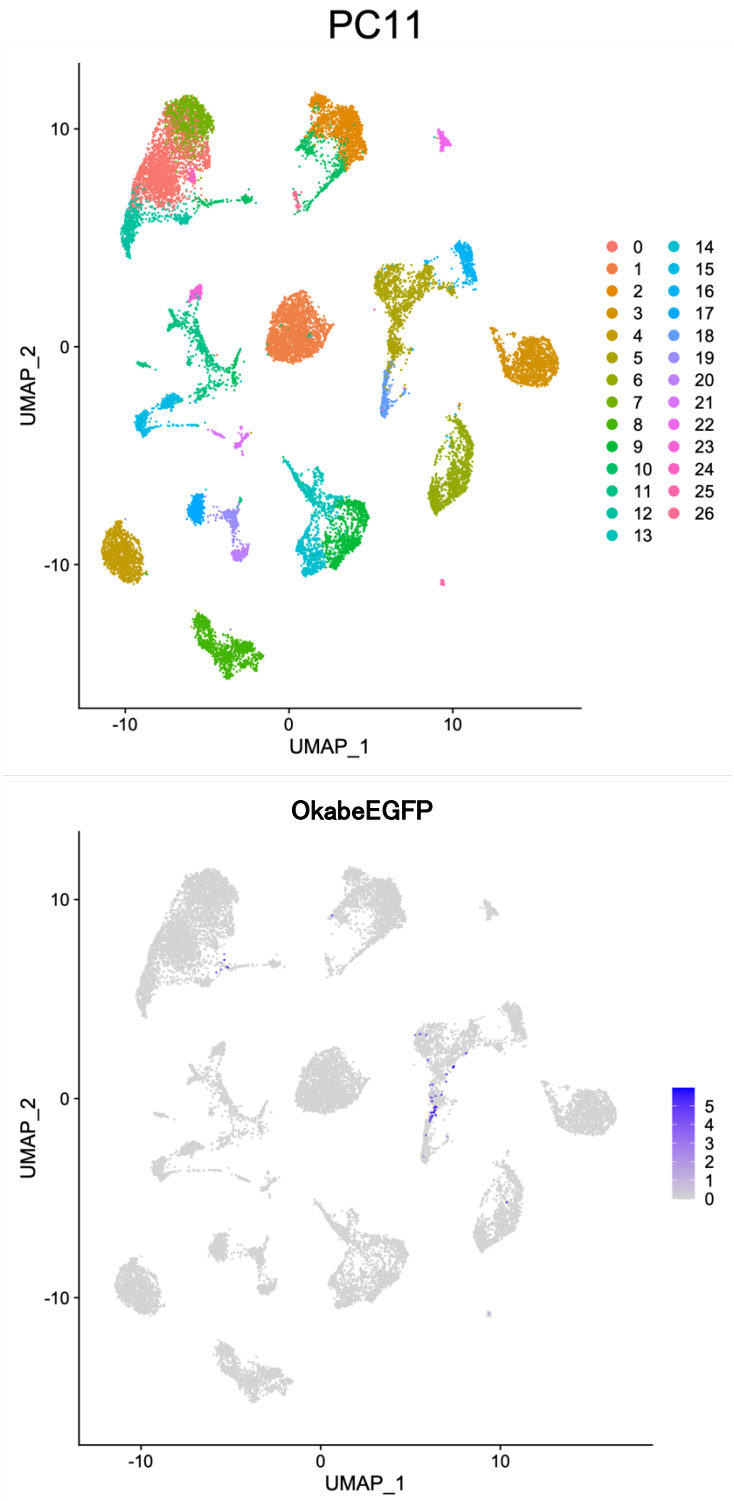

Fig. 20 Results of clustering with 11 PCs. The result indicates that all samples can be classified in 27 clusters (0 – 26). In this condition, MMc cells expressing OkabeEGFP were clustered in the cluster 0, 5, 6, 8, 10, 11,12, 18, 19, 22, and 25 as shown in the bottom panel (see also Table 8).

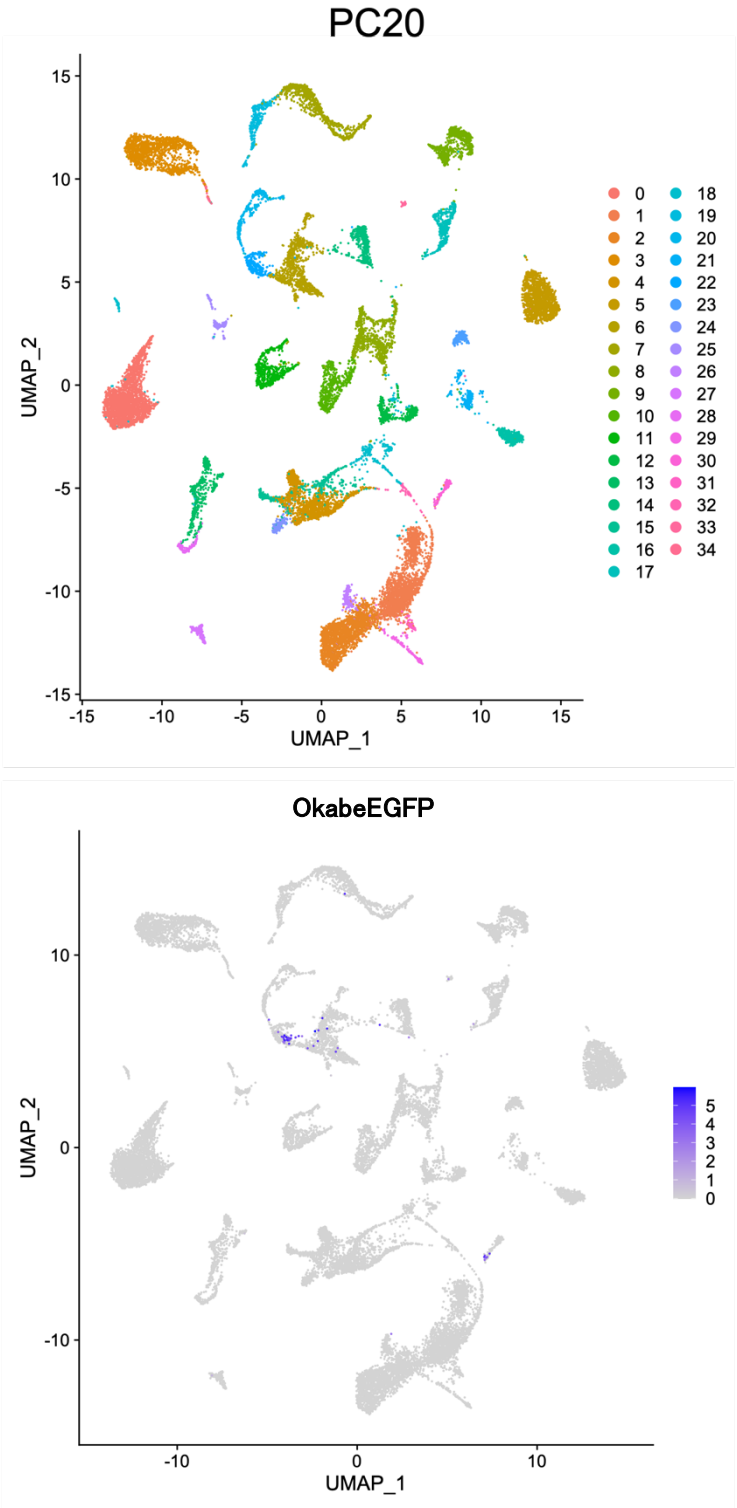

Fig. 21 Results of clustering with 20 PCs. The result indicates that all samples can be classified in 35 clusters (0 – 34). In this condition, MMc cells expressing OkabeEGFP were clustered in the cluster 6, 7, 8, 14, 15,17, 18, 21, 22, 26, 27, 29, 30, and 33 as shown in the bottom panel (see also Table 9).

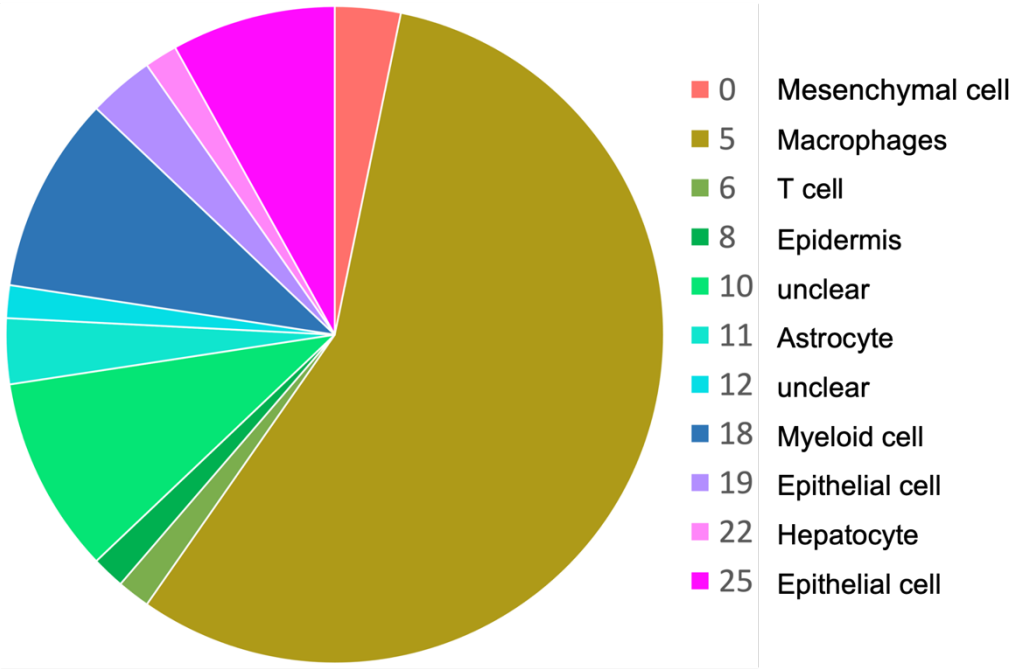

Fig. 22 Estimated major cell type of MMc cells of each cluster. 'Unclear' is the group of cells which were not estimated from the cell type of Tabula Muris cell samples.

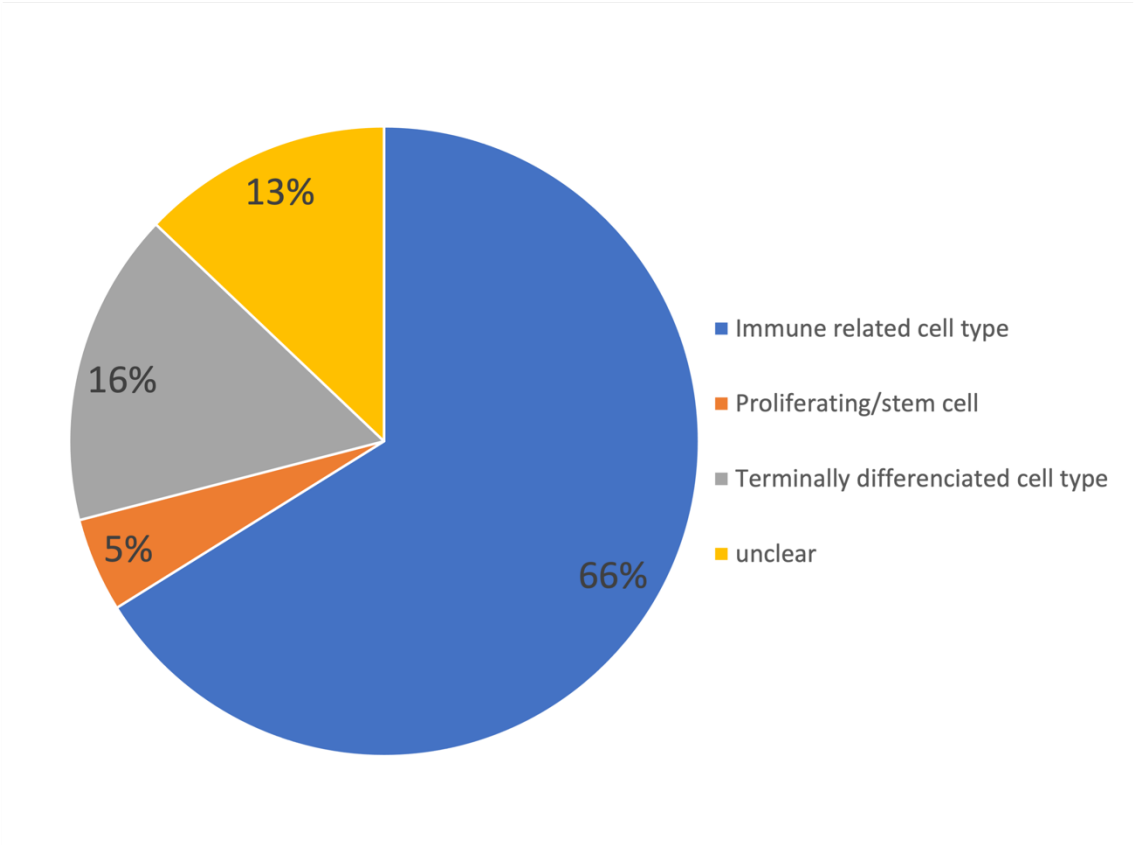

Fig. 23 Categorized MMc cell types and its ratio in MMc cell population.

Table 6 List of organ and its cell number of Tabula Muris (female mice).

Organs	cell number
Aorta	85
Bladder	389
Brain_Myeloid	2204
Brain_Non-Myeloid	705
Diaphragm	423
Fat	2146
Heart	2472
Kidney	192
Large_Intestine	1944
Limb_Muscle	517
Liver	161
Lung	914
Mammary_Gland	2405
Marrow	1632
Pancreas	719
Skin	696
Spleen	622
Thymus	664
Tongue	402
Trachea	582
(blank)	713
Total	**20587**

Table 7 List of cell type and its cell number of Tabula Muris (female mice).

Cell types	Cell number
astrocyte	91
B cell	772
basal cell	1340
basal cell of epidermis	530
basophil	12
Bergmann glial cell	8
bladder cell	174
bladder urothelial cell	215
blood cell	103
brain pericyte	28
Brush cell of epithelium proper of large intestine	36
cardiac muscle cell	74
ciliated columnar cell of tracheobronchial tree	14
classical monocyte	38
common lymphoid progenitor	7
DN1 thymic pro-T cell	26
endocardial cell	116
endothelial cell	1422
enterocyte of epithelium of large intestine	426
enteroendocrine cell	30
epidermal cell	90
epithelial cell	85
epithelial cell of large intestine	957
epithelial cell of lung	62
epithelial cell of proximal tubule	62
erythrocyte	14
fibroblast	1354
granulocyte	210
granulocyte monocyte progenitor cell	68
granulocytopoietic cell	35
hematopoietic precursor cell	4
hepatocyte	161
immature B cell	124
immature natural killer cell	19
immature NK T cell	18
immature T cell	618
keratinocyte	80
keratinocyte stem cell	383
kidney collecting duct epithelial cell	49
large intestine goblet cell	495

late pro-B cell	70
leukocyte	264
luminal epithelial cell of mammary gland	578
lung endothelial cell	421
lymphocyte	38
macrophage	163
mature natural killer cell	9
megakaryocyte-erythroid progenitor cell	8
mesenchymal cell	375
mesenchymal stem cell	256
mesenchymal stem cell of adipose	885
microglial cell	2185
monocyte	126
myeloid cell	647
myofibroblast cell	48
naive B cell	286
natural killer cell	79
neuron	36
oligodendrocyte	252
oligodendrocyte precursor cell	42
pancreatic A cell	185
pancreatic acinar cell	95
pancreatic D cell	46
pancreatic ductal cell	56
pancreatic PP cell	32
pancreatic stellate cell	12
pre-natural killer cell	7
precursor B cell	158
professional antigen presenting cell	9
regulatory T cell	12
skeletal muscle satellite cell	274
skeletal muscle satellite stem cell	213
Slamf1-negative multipotent progenitor cell	372
Slamf1-positive multipotent progenitor cell	4
smooth muscle cell	22
stem cell of epidermis	13
stromal cell	598
T cell	297
type B pancreatic cell	260
(Blank)	804
Total	**20587**

Table 8 MMc cell number identified in each cluster of UMAP with 11 PCs.

Cluster#	Cell number
0	2
5	35
6	1
8	1
10	6
11	2
12	1
18	6
19	2
22	1
25	5
Total	**62**

Table 9 MMc cell number identified in each cluster of UMAP with 20 PCs.

Cluster #	Cell number
6	8
7	1
8	1
14	6
15	1
17	1
18	1
21	2
22	31
26	1
27	1
29	1
30	6
33	1
Total	**62**

Table 10 List of cell type with the highest number of cells in each cluster of clustering with 11 PCs.

Cluster#	Cell type with the highest number of cells in each cluster
0	fibroblast
1	microglial cell
2	endothelial cell
3	B cell
4	basal cell
5	myeloid cell
6	immature T cell
7	mesenchymal stem cell of adipose
8	basal cell of epidermis
9	epithelial cell of large intestine
10	endothelial cell
11	astrocyte
12	skeletal muscle satellite cell
13	epithelial cell of large intestine
14	large intestine goblet cell
15	type B pancreatic cell
16	Slamf1-negative multipotent progenitor cell
17	luminal epithelial cell of mammary gland
18	granulocyte
19	luminal epithelial cell of mammary gland
20	bladder urothelial cell
21	pancreatic acinar cell
22	hepatocyte
23	oligodendrocyte
24	stromal cell
25	epithelial cell of lung
26	cardiac muscle cell

Table 11 List of cell types with the highest number of cells in each cluster of clustering with 20 PCs.

Cluster#	Cell type with the highest numbero of cells in each cluster
0	microglial cell
1	fibroblast
2	mesenchymal stem cell of adipose
3	B cell
4	endothelial cell
5	basal cell
6	myeloid cell
7	immature T cell
8	epithelial cell of large intestine
9	keratinocyte stem cell
10	enterocyte of epithelium of large intestine
11	large intestine goblet cell
12	type B pancreatic cell
13	astrocyte
14	Slamf1-negative multipotent progenitor cell
15	endothelial cell
16	luminal epithelial cell of mammary gland
17	basal cell of epidermis
18	epithelial cell of proximal tubule
19	immature T cell
20	granulocyte
21	luminal epithelial cell of mammary gland
22	monocyte
23	bladder urothelial cell
24	endothelial cell
25	pancreatic acinar cell
26	bladder cell
27	hepatocyte
28	oligodendrocyte
29	mesenchymal cell
30	myofibroblast cell
31	stromal cell
32	cardiac muscle cell
33	epithelial cell of lung
34	late pro-B cell

Chapter 5　General Discussion

5.1 Number of MMc cells in a whole embryo

MMc cells have been reported to be involved in various phenomena, such as immune tolerance, tissue regeneration and inflammatory diseases. From previous studies, the frequency of MMc cells seems to differ not only among different cases but also among patients with the same disease or even among control groups (6)(26). However, no research so far counted MMc cell number differences among individuals in healthy pregnancy. The present study tackled this issue for the first time, and suggested that MMc cell number differs between individuals, even in healthy pregnancy. As shown in Chapter 3, I counted the number of MMc cells from whole mouse embryos by developing a method described in Chapter 2 and by detecting GFP^+ cells. While I found that majority of the embryos showed a comparable number of MMc cells, around 3.7 cells / 10^7 sorted cells for those detected with GFP^+ cells (Fig 15, Table 5), an unexpected finding was that one of the embryos at the latest stage (E18.5) showed 1,816 cells/10^7 cells, which corresponds to a frequency approximately 500 times higher than that in the detected embryos (average 3.7 cells/ 10^7). The result suggests that while most of the embryos have a comparable number of MMc cells, a much higher count can be detected in some rare cases, and this difference could lead to various phenomena depending on additional factors such as the tolerance induction level.

Not only during the embryonic period, but also during the lactation period, MMc cell migration occurs (5)(51). Until the end of these periods, it is considered that the number of MMc cells would differ among individuals, and this difference might lead to various phenomena depending on the tolerance induction level. One possible explanation for this

idea is that the higher number of MMc cells introduce tolerance to NIMA. Some studies about organ transplants showed that the prognosis were well with higher levels of MMc cells (43). In addition, when the number of MMc cells is increased, maternal MHC-antigen complex can be transported into the child's dendritic cells by the dendritic cells of maternal origin and this can suppress the child's T cell activity (30).

Even though I could detect MMc cells as GFP positive cell in this study, there still remain technical difficulties. First is the fluorescence detection sensitivity of FACS, as it automatically removes cells as electronic aborts around 1 in 100 counts in my experiments. Having said so, FACS is more suitable for this experiment than microscopy, as it has higher sensitivity and have higher through put. Second, although we succeeded in isolating MMc cells from whole mice embryo, there could be a bias in the isolated cell types as isolation efficiency may differ among different tissues and cell types. Actually, some cell types, such as hepatocytes (37), are known to be fragile to flow sorting, and tends to be the most MMc cell detectable organs (52). In the meanwhile, with unknown reasons, only one cell was identified as liver-related MMc cell in my study. Finally, major caveats of this methodology would be that 7 – 8 hours are needed to process embryos to obtain single-celled suspension, and this could have biased the cell type repertoire based on their viability during the procedure.

5.2 Variety of MMc cell types in a whole embryo

In many previous studies, researchers have focused on immune related cells rather than

other cell types because MMc cells are non-self antigens for offspring and it has been considered that MMc cells have immunological influence on child. Therefore, there is no research elucidating the whole cell type repertoire of MMc cell population. In this study, I successfully isolated and analyzed 62 *GFP* expressing female cells as MMc cell from two whole mouse embryos. From this result, I estimated the cell types of each single MMc cells from their gene expression pattern and found that around 66% of the population is occupied by immune related cell types, but there are still 16% of terminally differentiated tissue specific cell types, such as hepatocyte, astrocyte and epidermis. In addition, about 5% of the population was expressing the genes of proliferating or mesenchymal stem cells. These results suggest that not only immune related cells, but also other cells are included as MMc cells.

To our knowledge, it is the first time revealing the MMc cell type repertoire of a whole mouse embryo. From my results, it seems that there are some cell types as small groups in the MMc cell population, such as stem cells or tissue specific cells. Given this, when a large number of MMc cells are migrated into the fetus, there is an increased chance that cells from the minor MMc cell types will be included. Having said so, it is still unclear if a very small number of specific cell types are important for feto-maternal tolerance induction, or simply the number of migrating MMc cells matters for the tolerance. With this regard, further studies are awaited in the future, preferably with more numbers of detected maternal cells, and further developed experimental systems that can control cell types and cell numbers which migrate into the fetus.

5.3 Relationships between MMc cells and various phenomena

In order to further investigate the relationships between MMc cells and various phenomena, it is necessary to conduct an animal experiment that can control both the cell types and the number of MMc cells. With this perspective, I will discuss three types of potential experimental ideas, especially for the embryonic period. First, investigating the cell number and cell type differences between fetus from healthy pregnancy and fetus from *Ly6e* or *Ifitm3* KO female mice, since these genes are not only known to be involved in cell migration, but were identified in all the isolated MMc cells. Provided MMc cells use these proteins play a crucial role in MMc cell migration from mother to fetus, the number of MMc cell should decrease in the fetus of the KO mother mice. Not only these KO mice, there are reports showing the changes on cell number under specific situations, as I will explain in the following sentences. Second idea is that investigating the cell types of MMc cell when the inflammatory stimulation was administered into the mother. This is based on the study by J. Wienecke *et al.* which showed treatment of Pertussis Toxin to pregnant mother resulted in a 3-fold increase in the migration of effector Th17 cells into the fetus (53), suggesting that regulation of inflammatory status in the mother could contribute to the cell type and cell number control. Lastly, it is also known that increased number of MMc cells migrates when the fetus has severe combined immunodeficiency (13). Although this is severe disease condition, this could be also one possible animal experimental system for investigating the maternal cell type and cell number migrated into fetus. Finally, my study showed the first evidence that MMc cell population includes not only immune related cell types but also stem

cell and differentiated tissue specific cell types. These various cell types migrate into fetus at relatively early phase of development. Considering that the number of migrating cells increases during pregnancy and there is still chance to get MMc cells via breast milk, my study showed the importance to figure out the repertoire of MMc cell population for understanding the biological importance of MMc cells, although it is still required to see MMc cell population of other mice embryos for discussing whether the population differs between individuals or not. Moreover, cell type estimation from its gene expression pattern would lead to revealing new function of MMc cells. If there are some MMc cell types, which has been ignored based on its function, it should lead to studies not only in immunology or medical fields, but also in developmental biology. In other words, it has been thought that MMc cells are minor cell population of mammals, but MMc cells can be said as cell level epigenetics and they would be recognized as novel constituents for offspring's development or health.

Acknowledgements

I would like to express my deepest and sincere gratitude to my supervisor, Dr. Naoki Irie (The University of Tokyo) for providing me with the opportunity to study about microchimerism in a splendid environment.

I would like to express my sincere appreciation to Dr. Shohei Hori (The University of Tokyo) and Dr. Akira Nakajima (The University of Tokyo) for the collaboration, the generous help about the experimental plan and discussion of my results. Especially, I could constructed the experimental design of the cell dissociation, cell sorting, and MACS part in Chapter 2, 3 and 4. Without their help, I could not even start my experiments, and my dissertation would not have been materialized.

I would also like to express my gratitude to Ms. Yumiko Tanaka (The University of Tokyo), Dr. Yoshitaka Shirasaki (The University of Tokyo), and Dr. Sotaro Uemura (The University of Tokyo) for conduction of single cell RNA-seq on small number of cells in Chapter 4. Without their help, I could not put the idea of MMc cell type estimation experiment into practice.

I would also like to express my gratitude to Dr. Etsuo A Susaki (Juntendo University) and Ms. Chika Shimizu (RIKEN Center for Biosystems Dynamics Research) for conduction of the transparent and immunostaining experiment in Chapter 2.

I am truly grateful to the member of Takeda Laboratory (the Laboratory of embryology, Department of Biological Sciences, Graduate School of Science, The University of Tokyo). I received a lot of advice from the members, especially Dr. Toru Kawanishi, Mr. Takafumi Ikeda and Mr. Jason Cheok Kuan Leong.

Some parts of experiments using FACS in this work was performed at One-stop Sharing Facility Center for Future Drug Discoveries in Graduate School of Pharmaceutical Sciences, the University of Tokyo. Sequencing of single cell RNA-seq was conducted by Life Science Data Research Center (LiSDaC). Lastly, I acknowledge one of the reviewers of the paper; "Whole embryonic detection of maternal microchimeric cells highlights significant differences in their numbers among individuals" (38) for providing a specific idea for discriminating maternal cells from cells of siblings.

References

1. Loubière LS, Lambert NC, Flinn LJ, Erickson TD, Yan Z, Guthrie KA, et al. Maternal microchimerism in healthy adults in lymphocytes, monocyte/macrophages and NK cells. Lab Investig. 2006;86(11):1185–92.

2. Pollack MS, Kirkpatrick D, Kapoor N, Dupont B, O'Reilly RJ. Identification by HLA Typing of Intrauterine-Derived Maternal T Cells in Four Patients with Severe Combined Immunodeficiency. N Engl J Med [Internet]. 1982 Sep 9;307(11):662–6. Available from: https://doi.org/10.1056/NEJM198209093071106

3. Geha RS, Reinherz E. Identification of circulating maternal T and B lymphocytes in uncomplicated severe combined immunodeficiency by HLA typing of subpopulations of T cells separated by the fluorescence-activated cell sorter and of Epstein Barr virus-derived B cell lines. J Immunol (Baltimore, Md 1950) [Internet]. 1983;130(6):2493–5. Available from: http://www.ncbi.nlm.nih.gov.proxy.kib.ki.se/pubmed/6304187

4. Kinder JM, Stelzer IA, Arck PC, Way SS. Immunological implications of pregnancy-induced microchimerism. Nat Reviwe Immunol [Internet]. 2017;17:483–94. Available from: http://dx.doi.org/10.1038/nri.2017.38

5. Aydın MŞ, Yiğit EN, Vatandaşlar E, Erdoğan E, Öztürk G. Transfer and Integration of Breast Milk Stem Cells to the Brain of Suckling Pups. Sci Rep. 2018;8(14289):1–9.

6. Nelson JL, Gillespie KM, Lambert NC, Stevens AM, Loubiere LS, Rutledge JC, et al. Maternal microchimerism in peripheral blood in type 1 diabetes and pancreatic islet beta cell microchimerism. Proc Natl Acad Sci USA [Internet]. 2007;104(5):1637–42. Available from: http://dx.doi.org/10.1073/pnas.0606169104

7. VanZyl B, Planas R, Ye Y, Foulis A, de Krijger RR, Vives-Pi M, et al. Why are levels of maternal microchimerism higher in type 1 diabetes pancreas? Chimerism. 2010;1(2):1–6.

8. Boddy AM, Fortunato A, Wilson Sayres M, Aktipis A. Fetal microchimerism and maternal health: A review and evolutionary analysis of cooperation and conflict beyond the womb. BioEssays. 2015;37(10):1106–18.

9. Desai RG, Creger WP. Maternofetal Passage of Leukocytes and Platelets in Man. Blood. 1963;21(6):665–73.

10. Kanaan SB, Gammill HS, Harrington WE, De SC, Stevenson PA, Forsyth AM, et al. Maternal microchimerism is prevalent in cord blood in memory T cells and other cell subsets , and persists post-transplant. Oncoimmunology [Internet]. 2017;6(5):1–10. Available from: https://doi.org/10.1080/2162402X.2017.1311436

11. Ariga H, Ohto H, Busch MP, Imamura S, Watson R, Reed W, et al. Kinetics of fetal cellular and cell-free DNA in the maternal circulation during and after pregnancy: Implications for noninvasive prenatal diagnosis. Transfusion. 2001;41(12):1524–30.

12. Sunami R, Komuro M, Tagaya H, Hirata S. Migration of microchimeric fetal cells into maternal circulation before placenta formation. Chimerism. 2010;1(2):66–8.

13. Piotrowski P, Croy B a. Maternal cells are widely distributed in murine fetuses in utero. Biol Reprod. 1996;54(5):1103–10.

14. Vernochet C, Caucheteux SM, Kanellopoulos-Langevin C. Bi-directional Cell Trafficking Between Mother and Fetus in Mouse Placenta. Placenta [Internet]. 2007;28(7):639–49. Available from: http://dx.doi.org/10.1016/j.placenta.2006.10.006

15. Molès J-P, Tuaillon E, Kankasa C, Bedin A-S, Nagot N, Marchant A, et al. Breastmilk cell trafficking induces microchimerism-mediated immune system maturation in the infant. Pediatr Allergy Immunol [Internet]. 2018;(November):1–11. Available from: http://doi.wiley.com/10.1111/pai.12841

16. Ninkina N, Kukharsky MS, Hewitt M V., Lysikova EA, Skuratovska LN, Deykin A V., et al. Stem cells in human breast milk. Hum Cell [Internet]. 2019;32(3):223–30. Available from: http://dx.doi.org/10.1007/s13577-019-00251-7

17. Stevens AM. Maternal microchimerism in health and disease. Best Pract Res Clin Obstet Gynaecol [Internet]. 2016;31:121–30. Available from: http://dx.doi.org/10.1016/j.bpobgyn.2015.08.005

18. Dutta P, Burlingham WJ. Stem cell microchimerism and tolerance to non-inherited maternal antigens. Chimerism. 2010;1(1):2–10.

19. Kinder JM, Jiang TT, Ertelt JM, Xin L, Strong BS, Shaaban AF, et al. Cross-Generational Reproductive Fitness Enforced by Microchimeric Maternal Cells. Cell [Internet]. 2015;162(3):505–15. Available from: http://dx.doi.org/10.1016/j.cell.2015.07.006

20. Ichinohe T, Uchiyama T, Shimazaki C, Matsuo K, Tamaki S, Hino M, et al. Feasibility of HLA-haploidentical hematopoietic stem cell transplantation between noninherited maternal antigen (NIMA)-mismatched family members linked with long-term fetomaternal microchimerism. Blood. 2004;104(12):3821–8.

21. Van Rood JJ, Loberiza FR, Zhang MJ, Oudshoorn M, Claas F, Cairo MS, et al. Effect of tolerance to noninherited maternal antigens on the occurrence of graft-versus-host disease after bone marrow transplantation from a parent or an HLA-haploidentical sibling. Blood. 2002;99(5):1572–7.

22. Iwai S, Okada A, Sasano K, Endo M, Yamazaki S, Wang X, et al. Controlled induction of immune tolerance by mesenchymal stem cells transferred by maternal microchimerism. Biochem Biophys Res Commun [Internet]. 2021;539:83–8. Available from: https://doi.org/10.1016/j.bbrc.2020.12.032

23. Saadai P, MacKenzie TC. Increased maternal microchimerism after open fetal surgery. Chimerism. 2012;3(3):1–3.

24. Ye J, Vives-Pi M, Gillespie KM. Maternal microchimerism: Increased in the insulin positive compartment of type 1 diabetes pancreas but not in infiltrating immune cells or replicating islet cells. PLoS One. 2014;9(1):e86985.

25. Muraji T, Suskind DL, Irie N. Biliary atresia: A new immunological insight into etiopathogenesis. Expert Rev Gastroenterol Hepatol. 2009;3(6):599–606.

26. Muraji T, Hosaka N, Irie N, Yoshida M, Imai Y, Tanaka K, et al. Maternal microchimerism in underlying pathogenesis of biliary atresia: quantification and phenotypes of maternal cells in the liver. Pediatrics [Internet]. 2008;121(3):517–21. Available from: http://www.ncbi.nlm.nih.gov/pubmed/18310200

27. Irie N, Muraji T, Hosaka N, Takada Y, Sakamoto S, Tanaka K. Maternal HLA class I compatibility in patients with biliary atresia. J Pediatr Gastroenterol Nutr. 2009;49(4):488–92.

28. Roy E, Leduc M, Guegan S, Rachdi L, Kluger N, Scharfmann R, et al. Specific maternal microchimeric T cells targeting fetal antigens in b cells predispose to auto-immune diabetes in the child. J Autoimmun [Internet]. 2011;36(3–4):253–62. Available from: http://dx.doi.org/10.1016/j.jaut.2011.02.003

29. Leveque L, Hodgson S, Peyton S, Koyama M, MacDonald KPA, Khosrotehrani K. Selective organ specific inflammation in offspring harbouring microchimerism from strongly alloreactive mothers. J Autoimmun [Internet]. 2014;50:51–8. Available from: http://dx.doi.org/10.1016/j.jaut.2013.10.005

30. Bracamonte-Baran W, Florentin J, Zhou Y, Jankowska-Gan E, Haynes WJ, Zhong W, et

al. Modification of host dendritic cells by microchimerism-derived extracellular vesicles generates split tolerance. Proc Natl Acad Sci [Internet]. 2017;114(5):201618364. Available from: http://www.pnas.org/lookup/doi/10.1073/pnas.1618364114

31. WILLIAM J. BURLINGHAM, PH.D., ALAN P. GRAILER, M.S.,* DENNIS M. HEISEY, PH.D., FRANS H.J. CLAAS, PH.D., DOUGLAS NORMAN, M.D., THALACHALLOUR MOHANAKUMAR, PH.D., DANIEL C. BRENNAN, M.D., HANS DE FIJTER, M.D., TEUN VAN GELDER, M.D., JOHN D. PIRSCH, M.D., HAN MD. The Effect of Tolerance To Noninherited Maternal HLA Antigens on the Survival of Renal Transplants From Sibling Donors. N Engl J Med. 1998;339(23):1657–64.

32. Okabe M, Ikawa M, Kominami K, Nakanishi T, Nishimune Y. "Green mice" as a source of ubiquitous green cells. FEBS Lett [Internet]. 1997;407(3):313–9. Available from: http://dx.doi.org/10.1016/S0014-5793(97)00313-X

33. Mass E, Ballesteros I, Farlik M, Halbritter F, Günther P, Crozet L, et al. Specification of tissue-resident macrophages during organogenesis. Science (80-). 2016;353(aaf4238).

34. Susaki EA, Tainaka K, Perrin D, Yukinaga H, Kuno A, Ueda HR. Advanced CUBIC protocols for whole-brain and whole-body clearing and imaging. Nat Protoc [Internet]. 2015;10(11):1709–27. Available from: http://dx.doi.org/10.1038/nprot.2015.085

35. Susaki EA, Shimizu C, Kuno A, Tainaka K, Li X, Nishi K, et al. Versatile whole-organ/body staining and imaging based on electrolyte-gel properties of biological tissues. Nat Commun. 2020;11(1).

36. Jeanty C, Derderian SC, Mackenzie TC. Maternal-fetal cellular trafficking: Clinical implications and consequences. Curr Opin Pediatr. 2014;26(3):377–82.

37. MacParland SA, Liu JC, Ma XZ, Innes BT, Bartczak AM, Gage BK, et al. Single cell RNA

sequencing of human liver reveals distinct intrahepatic macrophage populations. Nat Commun. 2018;9(1):1–21.

38. Fujimoto K, Nakajima A, Hori S, Irie N. Whole embryonic detection of maternal microchimeric cells highlights significant differences in their numbers among individuals. PLoS One [Internet]. 2021;16(12):e0261357. Available from: http://dx.doi.org/10.1371/journal.pone.0261357

39. Picelli S, Björklund ÅK, Faridani OR, Sagasser S, Winberg G, Sandberg R. Full-length RNA-seq from single cells using Smart-seq2. Nat Protoc. 2014;9(1):171–81.

40. Schaum N, Karkanias J, Neff NF, May AP, Quake SR, Wyss-Coray T, et al. Single-cell transcriptomics of 20 mouse organs creates a Tabula Muris. Nature. 2018;562(7727):367–72.

41. Ki S, Park D, Selden HJ, Seita J, Chung H, Kim J, et al. Global transcriptional profiling reveals distinct functions of thymic stromal subsets and age-related changes during thymic involution. Cell Rep [Internet]. 2014;9(1):402–15. Available from: http://dx.doi.org/10.1016/j.celrep.2014.08.070

42. Stern M, Ruggeri L, Mancusi A, Bernardo ME, De Angelis C, Bucher C, et al. Survival after T cell depleted haploidentical stem cell transplantation is improved using the mother as donor. Blood. 2008;112(7):2990–5.

43. Nijagal A, Fleck S, Hills NK, Feng S, Tang Q, Kang SM, et al. Decreased risk of graft failure with maternal liver transplantation in patients with biliary atresia. Am J Transplant. 2012;12(2):409–19.

44. Araki M, Hirayama M, Azuma E, Kumamoto T, Iwamoto S, Toyoda H, et al. Prediction of Reactivity to Noninherited Maternal Antigen in MHC-Mismatched, Minor

Histocompatibility Antigen-Matched Stem Cell Transplantation in a Mouse Model. J Immunol. 2010;185(12):7739–45.

45. Asundi J, Crocker L, Tremayne J, Chang P, Sakanaka C, Tanguay J, et al. An antibody-drug conjugate directed against lymphocyte antigen 6 complex, locus E (LY6E) provides robust tumor killing in a wide range of solid tumor malignancies. Clin Cancer Res. 2015;21(14):3252–62.

46. Lv Y, Song Y, Ni C, Wang S, Chen Z, Shi X, et al. Overexpression of Lymphocyte Antigen 6 Complex, Locus e in Gastric Cancer Promotes Cancer Cell Growth and Metastasis. Cell Physiol Biochem. 2018;45(3):1219–29.

47. Tanaka SS, Yamaguchi YL, Tsoi B, Lickert H, Tam PPL. IFITM/mil/fragilis family proteins IFITM1 and IFITM3 play distinct roles in mouse primordial germ cell homing and repulsion. Dev Cell. 2005;9(6):745–56.

48. Hou Y, Wang S, Gao M, Chang J, Sun J, Qin L, et al. Interferon-Induced Transmembrane Protein 3 Expression Upregulation Is Involved in Progression of Hepatocellular Carcinoma. Biomed Res Int. 2021;2021.

49. Chen C-P, Lee M-Y, Huang J-P, Aplin JD, Wu Y-H, Hu C-S, et al. Trafficking of multipotent mesenchymal stromal cells from maternal circulation through the placenta involves vascular endothelial growth factor receptor-1 and integrins. Stem Cells. 2008;26(2):550–61.

50. Unno A, Suzuki K, Kitoh K, Takashima Y. Fetally Derived CCL3 is Not Essential for the Migration of Maternal Cells Across the Blood–Placental Barrier in the Mouse. J Vet Med Sci. 2010;72(11):1399–403.

51. Hassiotou F, Beltran A, Chetwynd E, Stuebe AM, Twigger AJ, Metzger P, et al.

Breastmilk is a novel source of stem cells with multilineage differentiation potential. Stem Cells. 2012;30(10):2164–74.

52. Dutta P, Molitor-Dart M, Bobadilla JL, Roenneburg DA, Yan Z, Torrealba JR, et al. Microchimerism is strongly correlated with tolerance to noninherited maternal antigens in mice. Blood. 2009;114(17):3578–87.

53. Wienecke J, Hebel K, Hegel KJ, Pierau M, Brune T, Reinhold D, et al. Pro-inflammatory effector Th cells transmigrate through anti-inflammatory environments into the murine fetus. Placenta [Internet]. 2012;33(1):39–45. Available from: http://dx.doi.org/10.1016/j.placenta.2011.10.014